TRIBHUVAN UNIVERSITY

INSTITUTE OF ENGINEERING

PULCHOWK CAMPUS

THESIS NO.: M-84-MSMDE-2020-2024

Burst Strength Analysis of an LPG Cylinder using Experiment Data and Numerical Simulation

by

Chandra Bhushan Yadav

A THESIS

SUBMITTED TO THE DEPARTMENT OF MECHANICAL AND AEROSPACE ENGINEERING IN PARTIAL FULFILLMENT OF THE REQUIREMENTS FOR THE DEGREE OF MASTER OF SCIENCE IN MECHANICAL SYSTEMS DESIGN AND ENGINEERING

DEPARTMENT OF MECHANICAL AND AEROSPACE ENGINEERING

LALITPUR, NEPAL

JUNE, 2024

COPYRIGHT

TRIBHUVAN UNIVERSITY
INSTITUTE OF ENGINEERING
PULCHOWK CAMPUS
DEPARTMENT OF MECHANICAL AND AEROSPACE EGINEERING

The undersigned hereby certify that they have read, and recommended to the Institute of Engineering for acceptance, thesis entitled "**Burst Strength Analysis of an LPG Cylinder using Experiment and Numerical Simulation**" submitted by Chandra Bhushan Yadav in partial fulfillment of the requirements for the degree of Master of Science, Mechanical Systems Design and Engineering.

Supervisor, Nawraj Bhattarai, Ph.D.
Associate Professor
Department of Mechanical and Aerospace Engineering, Pulchowk Campus

----
Supervisor, Navin Kumar Jha
Assistant Professor
Department of Mechanical and Aerospace Engineering, Pulchowk Campus

----
External Examiner, Er. Rudra Mani Ghimire
Manager
Civil Aviation Authority of Nepal (CAAN)

Committee Chairman, Sudip Bhattrai, Ph.D.
Head of Department
Department of Mechanical and Aerospace Engineering, Pulchowk Campus

Tribhuvan University
Institute of Engineering
Department of Mechanical and Aerospace Engineering
Pulchowk Campus

Date: 9th June, 2024

ABSTRACT

The research focuses on assessing the burst strength of the 14.2 Kg LPG cylinders for which the model is prepared according to Nepal and Indian Standards. 2.61 mm is chosen as the thickness of the LPG cylinder for which the minimum internal pressure is calculated using the ASME BPVC Section VIII, Division 1 and Nepal Standard Code using the yield strength as the allowable stress limit. The yield and ultimate tensile strength are obtained from the uniaxial tensile tests, while burst pressure is obtained from the hydrostatic pressure burst test. The test conducted on 9 different LPG cylinder samples resulted in an average yield strength, ultimate tensile strength and burst pressure of 283.879, 421.045 and 8.72 MPa respectively.

The analytical burst pressure as per shell theory obtained is 6.98 MPa. Numerical simulation as per ASME BPVC Section VIII, Division 2, Part 5 yields burst pressure of 7.0014, 7.506713, and 8.421 MPa from Elastic, Limit Load and Elastic Plastic analysis respectively with, elastic plastic analysis considered most realistic approach. Since LPG cylinders are symmetrical about the longitudinal axis, axisymmetric 2D analysis is performed.

Principal stresses like hoop, axial and radial stresses are the most important classes of the stresses developed within the pressure vessels. The equivalent von-mises stress is calculated from these principal stresses and is compared with the failure criterion to determine the occurrence of the bursting of the LPG cylinders. However, in pressure vessels, the hoop stress is considered as the critical component as using the elastic plastic analysis, the maximum hoop and equivalent stress developed within the LPG cylinder at an internal burst pressure of 8.421 MPa is 616 and 551.03 MPa respectively, which shows that at this burst pressure the hoop stress is much larger than the equivalent von-mises stress developed.

ACKNOWLEDGEMENT

I would like to express my sincere gratitude to Associate Prof. Dr. Nawraj Bhattarai and Assistant Prof. Navin Kumar Jha, Pulchowk Campus for supervising my thesis work. Without their continuous support and guidance, this research would not have been completed.

I would like to express my deepest thanks to Assistant Prof. Dr. Sudip Bhattrai, Head of Department, Department of Mechanical and Aerospace Engineering. I would like to express sincere gratitude to Professor Dr. Laxman Poudel, Coordinator, M.Sc. in Mechanical Systems Design and Engineering for his treasured guidance throughout my academic journey. I am grateful for the valuable suggestions and kind support which I received from all the teachers and faculty members of the department during the time of my research.

I would like to take this opportunity to give special thanks to Mr. Sanjeev Kumar Thakur sir, Er. Sagar Baral from Nepal Bureau of Standards and Metrology for their helpful suggestions and technical guidance on my research. I am also thankful to all the staff members, especially Mr. Manoj Singh sir of the Arrowtech Private Limited at Birgunj, where I visited and got a chance to perform an experiment for my research which helped me a lot to prepare this thesis.

I express my thanks to Er. Bishesh Bhattarai for his valuable insight, which helped me throughout my research journey. I would also want to offer my heartfelt gratitude and appreciation to my parents, family members and friends for their unwavering support and constant source of inspiration during this thesis project.

Chandra Bhushan Yadav

076/MSMDE/005

TABLE OF CONTENTS

LIST OF FIGURES

LIST OF TABLES

LIST OF SYMBOLS

P, P_h	Internal Pressure
σ_H	Hoop Stress
σ_A	Axial Stress
r	Internal Radius
P_b	Burst pressure
S	Allowable stress
t	Thickness of the cylinder/pipe
D_1	Diameter of the cylinder/pipe.
σ_{ys}, Re	Yield Strength
σ_{ult}	Ultimate Strength
D_o	Outer diameter
D_i	Inner diameter
D	Inside diameter of the head skirt or inside length of major axis of ellipsoidal head.
E	Young's Modulus of Elasticity
ε	Strain
σ	Stress
v	Poisson's Ratio
G	Shear Modulus of Elasticity.
σ_{eng}	Engineering Stress
σ_{true}	True Stress

ε_{eng}	Engineering Strain
ε_{true}	True Strain
$\varepsilon_{plastic}$	Plastic Strain
ε_{total}	Total Strain
$\varepsilon_{elastic}$	Elastic Strain
P_b	Burst Pressure
a, b	Half of major and minor axis of the ellipsoidal head
S	Maximum allowable stress value
t	Minimum thickness of shell
P	Internal design pressure
E	Joint efficiency
R	Inside radius of the shell
t	Calculated minimum wall thickness,
J	Weld joint factor
h_o	External height of the domed ends
h_i	Internal height of the domed ends
K	Ratio D_o / h_o is the ratio of the major to minor axis
Sf	Length of straight flange

LIST OF ABBREVIATIONS

LPG	Liquefied Petroleum Gases
PV	Pressure Vessel
CAD	Computer Aided Design
FEM	Finite Element Method
BPVC	Boiler and Pressure Vessel Code
ASME	The American Society of Mechanical Engineers
NS	Nepal Standards
IS	Indian Standards
NOC	Nepal Oil Corporation
IOC	Indian Oil Corporation
SCL	Stress Classification Line
PT	Parent Tangential
PL	Parent Longitudinal
W	Weld
UTS	Ultimate Tensile Strength
DBR	Design by Rule
DBA	Design by Analysis
SVF	Short Vertical Fracture
LVF	Long Vertical Fracture

CHAPTER ONE: INTRODUCTION

1.1 Background

A pressure vessel is a closed container used to store liquids or gases at a pressure substantially higher or lower than the atmospheric pressure. As per ASME BPVC VIII - 1, 2015, pressure vessels are defined as “containers used for the containment of pressure, either internal or external”.

Liquified Petroleum Gas also known as LPG is a compressed gas that comprises of mainly two hydrocarbons propane (C_3H_8), butane (C_4H_{10}), and a small part of ethane (C_2H_6) or pentane (C_5H_{12}) (Setiyo et al., 2017). LPG has a liquefaction of about 270:1, i.e., as a gas, it expands 270 times its volume as a liquid (Fadel and Yahya, 2021). Thus, LPG are stored as a liquid in a pressurized containers at about 0.6 – 1.5 MPa (Adolf et al., 2015) which then transitions to a gas when the pressure is released. This characteristic facilitates transportation and storage as a liquid while enabling combustion as a gas.

Generally, LPG are stored in a cylindrical type pressure vessel and is increasingly employed as fuel for cooking, heating applications and also as an alternative fuel for internal combustion engines in vehicles. Its versatility extends to applications as an aerosol propellant and refrigerant, replacing chlorofluorocarbons to mitigate ozone layer damage. Since, LPG is highly flammable and odorless, it is mixed with an additive, ethyl mercaptan for leak detection, chosen for its non-corrosive nature, low sulfur content, and a boiling point closely aligned with that of LPG. When mixed with air, LPG can pose combustion or explosion risks upon encountering an ignition source. Being denser than air, LPG naturally descends to the ground.

Cylinders used for storing LPG, require materials with high tensile and compressive strength to withstand such high gas pressure. These cylinders are crucial for safely transporting hazardous LPG from bottler plants to end consumers. Though various national and international standards, codes and regulations govern the cylinder design, manufacturing, and usage, certain gaps exist in ensuring material safety and compliance. The Figure 1 shows a commercial LPG cylinder of capacity 14.2 Kg used in Nepali household.

[Image Source: Sujan Dhungana, 2016. Accessed via: https://myrepublica.nagariknetwork.com/news/noc-still-profits-rs-111-7-per-lpg-cylinder]

Figure 1: A typical 14.2 kg type LPG cylinder used in Nepali household

In our nation, safety of LPG cylinders is on rise as there are 6.5 million cylinders from 60 bottlers in circulation in the country, for which around 200,000 gas cylinders could be defective (The Kathmandu Post, 2016). Reports indicate a significant global toll of 265,000 lives lost in LPG gas cylinder fire-related incidents, with over fifty percent of these incidents occurring in South and Southeast Asia. Estimated data from 2008 suggests that around 55,000 individuals are annually affected by such fire-related incidents, and in Nepal, approximately 2,100 people lose their lives each year in such incidents. Kirtipur Hospital records from the past three years reveal that 134 people were admitted for the treatment of incidents related to gas explosion, resulting in 33 fatalities during hospitalization (The Kathmandu Post, 2023).

1.2 Statement of the Problem

LPG used in household application for cooking purposes normally are contained in a cylindrical type pressure vessel with capacity of 5 kg and 14.2 kg. These cylinders are made up of metallic materials like welded steel, aluminum or composite alloys which are highly prone to corrosion. Same old LPG cylinders are circulated in the market of which no proper information is provided which poses the risk of failure. The widespread usage of domestic Liquefied Petroleum Gas (LPG) cylinders as the primary source of fuel presents a potential safety concern due to instances of cylinder failures. In most of the cases, the failure of cylinders is due to the leakage of LPG and its contact with the sources of ignition, and in other cases, the reasons being unknown. So, ensuring the integrity and reliability of these cylinders is crucial for household safety, and it is essential to comprehend the underlying causes of failures for effective risk assessment and mitigation.

Recently, Nepal has witnessed a surge in LPG cylinder accidents, necessitating a safety risk assessment. Nepal Oil Corporation is the only one enterprises of Nepal that imports, stores and distributes various petroleum products in the country. Some of LPG cylinders used for household application are manufactured locally in Nepal. Test data such as LPG working pressure, burst pressure, metals properties such as yield and ultimate tensile strength are not available easily. There is a lack of local data and research regarding the LPG. Most of the researches that have been done are mainly based on the foreign context which may not be applied in context of Nepal. The absence of a comprehensive understanding of these failure mechanisms hampers the development of targeted safety measures and preventive strategies. In Nepal, FEA is not widely used. Further study is required to determine how to optimize LPG cylinder designs in Nepal using computational and finite element analysis (FEA) techniques.

1.3 Rationale of the Research

The research focuses on the safety and risk assessment of the LPG cylinders by studying its burst strength. The research will incorporate FEA techniques to study the failure analysis of LPG cylinders complying with the national and international codes such as Nepal Standards and ASME BPVC. The research aims to establish a methodology for the design, test and analysis of the LPG cylinders using computational methods complying with the national and international codes. Use of FEA and modern computational methods will lead to more efficient, cost and time-effective designs. Moreover, the research will help fulfill the gap of use of FEA methods and ensure that the industry professionals are well equipped and versed with these modern techniques in the design and analysis of LPG cylinders. The advantages of this research work can be summarized as:

1. Enhance Safety and Reliability
2. Modernize Testing and Design Methods regarding the LPG Cylinders
3. Fill Research and Data Gaps

1.4 Objective of the Research

1.4.1 Main Objective

- To perform the burst strength analysis of an LPG cylinder using finite element method to analyze the failure of 14.2 Kg LPG cylinders used in Nepal.

1.4.2 Specific Objectives

- To conduct experiments such as hydrostatic burst pressure tensile test to determine the material properties of the LPG cylinder.
- To check the compliance of the 14.2 Kg LPG cylinder design as per Nepal Standards.
- To run numerical simulations on ANSYS to predict the burst pressure of the LPG cylinder.
- To validate the experimental data with the simulation results and the analytical solutions.
- To study the various stress components such as equivalent, hoop, and longitudinal stress during the bursting.

1.5 Scopes and Limitations of the Research

In this research, the analysis of the 14.2 Kg LPG cylinder is carried out using the experimental, theoretical and FEA approaches. The experiment results are the most important data sources for the validation and verification of the methods used in the research work. The analytical calculation is based on the theories provided by the concepts of solid mechanics whereas the FEA is done following the literature provided in the part Desing by Analysis of the ASME BPVC Section VIII Division 2.

The assumption and limitation of the research are listed as follows:

- The research focuses only on the 14.2 kg LPG cylinders mainly used in Nepali household.
- The CAD model created is based on the drawing provided by NOC and IOC, considering shell and head portion of LPG cylinders only.
- The numerical solutions obtained are compared with the analytical solution based on the assumption of thin-walled vessel.
- In LPG cylinders, circumferential and longitudinal weld beads are present. However, in this research, the geometry of the LPG cylinder is simplified by not considering the weld beads.

- The vapor pressure of commercial butane-propane mixture at 65° C is around 10 – 26 Kgf/cm^2 (1 - 2.549 MPa) as per NS 370,2054, Specification for Liquefied Petroleum Gas (LPG). The study does not consider the effect of temperature on the vapor pressure of the LPG on the cylinder. The study considers that the LPG cylinder is kept at a normal temperature and pressure (NTP) condition for which the vapor pressure is around 0.215 – 0.85 MPa.

CHAPTER TWO: SYSTEM DESCRIPTION

2.1 Theoretical Background

Following sections provide the theories behind the design, analysis of pressure vessels and related literatures.

2.1.1 Pressure Vessel

A closed container designed to keep gases or liquids at a pressure significantly different from the surrounding air is known as Pressure Vessel. These vessels are commonly used in various industrial processes for storing, transporting, or processing substances under high pressure or vacuum conditions. Pressure vessels come in different shapes, such as cylindrical or spherical. Typically constructed from materials like carbon or stainless steel, these vessels are often assembled through welding. They play a crucial role in industries such as petrochemical, energy, and manufacturing, where the containment of pressurized substances is essential for specific processes or applications. Design and construction of pressure vessels adhere to established codes and standards to ensure safety and reliability in their operation. Pressure vessels employed in industrial applications serve as sealed containers resistant to leaks. They typically exhibit cylindrical or spherical shapes, featuring diverse head configurations.

Pressure vessels are classified based on the wall thickness, the shape and the function of the vessel. Pressure vessels are mainly categorized into two main categories:

1 Thin-walled pressure vessels

2 Thick-walled pressure vessels

When vessels are considered to be formed of plate in which the thickness is small as compared with other dimensions, and as such offer little resistance to the bending perpendicular to the surface, they are called membranes or shells (Harvey, 1985). A thin-walled pressure vessel has a small wall thickness as compared to the overall diameter of the shell. For a pressure vessel to be considered as a thin-walled, the wall thickness should be less than or equal to the 10% of the inner radius, i.e., $\frac{r}{t} \geq 10$. And for all other cases where the wall thickness is greater than 10% of the inner radius, it is considered as a thick-walled pressure vessel (Doane, 2018). The Figure 2 shows the distinction between the thin and thick-walled pressure vessel.

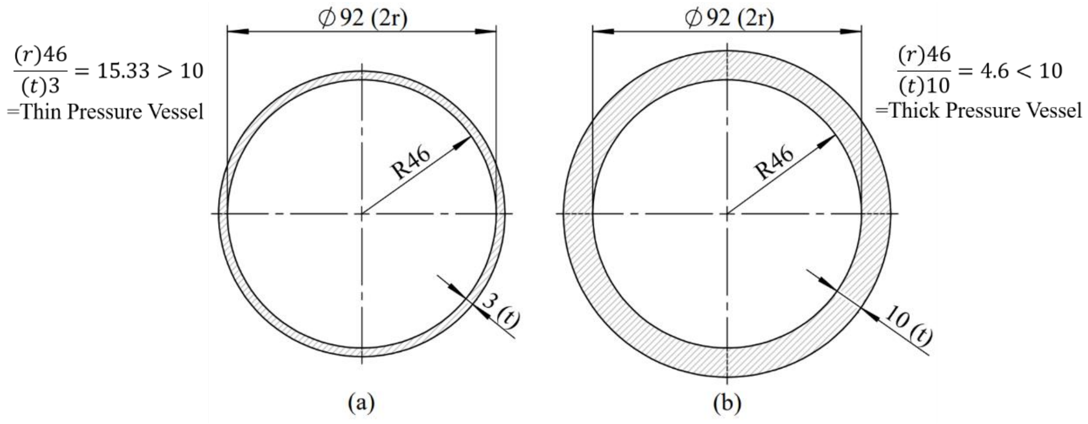

Figure 2: Pressure Vessel Section
(a): Thin-Walled, (b): Thick-Walled

Based on Shape, they are classified as:

1 **Cylindrical Pressure Vessel:**

Cylindrical pressure vessels, characterized by a cylinder-shaped shell with enclosures (heads) on each end, are widely favored for their affordability, ease of production, and adaptability across industries. Despite their common use, these vessels can be vulnerable at the points where the heads connect to the shell due to stress concentrations. However, this weakness can be addressed by employing thicker materials for the heads and adopting more rounded shapes, which aids in distributing stress more uniformly. Additional strengthening methods such as incorporating stiffening rings or weld pads further fortify these areas. Overall, cylindrical pressure vessels remain popular across various sectors like oil and gas, chemical processing, and manufacturing, owing to their simplicity and ability to accommodate diverse pressure and volume needs.

2 **Spherical Pressure Vessels:**

Another predominantly used type pressure vessel is spherical. Unlike cylindrical pressure vessels, spherical pressure vessels do not possess weak points because the internal and external pressure is uniformly distributed across the entire surface. However, the spherical design presents challenges in production due to its complexity and higher cost compared to cylindrical vessels. Despite this, spherical pressure vessels offer the advantage of evenly dispersing pressure, making them advantageous in certain applications despite their manufacturing drawbacks.

The Figure 3 shows a horizontal type cylindrical pressure vessel.

Figure 3: Pressure Vessels
[Image Source: apexge.com]

2.1.2 Pressure Vessel Formed Heads

Cylindrical Pressure vessels are again differentiated based on the use of formed heads to close the cylindrical shell. These are generally called end heads or end caps and are categorized as follows:

1. Flat Heads
2. Hemispherical Heads
3. Semi-Ellipsoidal Heads
4. Tori-spherical Heads
5. Conical Heads

Ellipsoidal, hemispherical and tori-spherical heads are generally most used heads in cylindrical pressure vessels. The Figure 4 shows the schematic of the formed heads used in cylindrical pressure vessels:

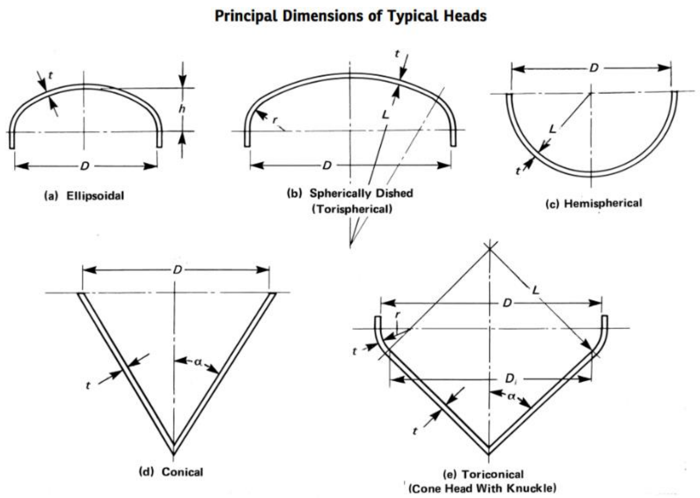

Figure 4: Different types of Heads used in Pressure Vessels
[Image Source: ASME BPVC.VIII.1-2015 Figure 1-4]

2.1.3 Stresses in Pressure Vessel

Pressure vessels commonly have the forms of spheres, cylinders, cones, ellipsoids, or some combination of these shapes. In general, pressure vessels are usually composed of a complete pressure containing shell in combination with flange rings and fasteners for connecting and securing. The main purpose of the pressure vessel is to withhold internal pressure or external pressure without crumbling down. These pressures are assumed to be uniform and perpendicular across the vessel surface. The vessels are subjected to membrane and bending stresses. For most of the cases, the bending stresses are neglected and only the major membrane stresses are considered for the design of the pressure vessels. However, in case of shape and material discontinuity, the bending stresses must be incorporated while designing the pressure vessels. The membrane stresses within a pressure vessel serves as a comprehensive measure, capturing the combined impact of various stress types acting on the material due to internal pressure. When a pressure vessel undergoes pressurization, it encounters multiple stress components, namely:

1. **Hoop Stress (Circumferential Stress):** Whenever a circular ring or a vessel is subjected to an internal pressure or external pressure uniformly distributed along its circumference, hoop forces will be produced throughout the thickness which act in the tangential direction. This will result in uniform enlargement of the ring or vessel if the pressure is internal, or contraction of the ring or vessel if the pressure is external. Hoop stress is widely recognized as the most critical stress in the majority of pressure vessel designs. For thin-walled cylindrical pressure vessel, hoop stress is given as:

   1. $$\sigma_{\mathrm{H}} = \frac{Pr}{t} \tag{2.1}$$

2. **Axial Stress (Longitudinal Stress):** Axial stress results from the axial (vertical) forces generated by the internal pressure and operates parallel to the longitudinal axis of the vessel. For thin-walled cylindrical pressure vessels, the axial stress is given as:

   1. $$\sigma_{\mathrm{A}} = \frac{Pr}{2t} \tag{2.2}$$

3. **Radial Stress:** Radial stress acts perpendicularly to the inner and outer surfaces of the vessel. However, it is often considered negligible when compared to hoop and axial stresses. While contributing to the overall stress profile, radial stress

is typically of lesser significance in pressure vessel designs. For thin-walled pressure vessel, the radial stress is generally considered to be equal to the internal pressure present.

Evaluating the equivalent stress involves considering the combined effects of hoop stress, axial stress, and, to a lesser extent, radial stress, providing a comprehensive perspective on the material's response to internal pressure within the pressure vessel. The Figure 5 shows the various stresses present in the pressure vessels.

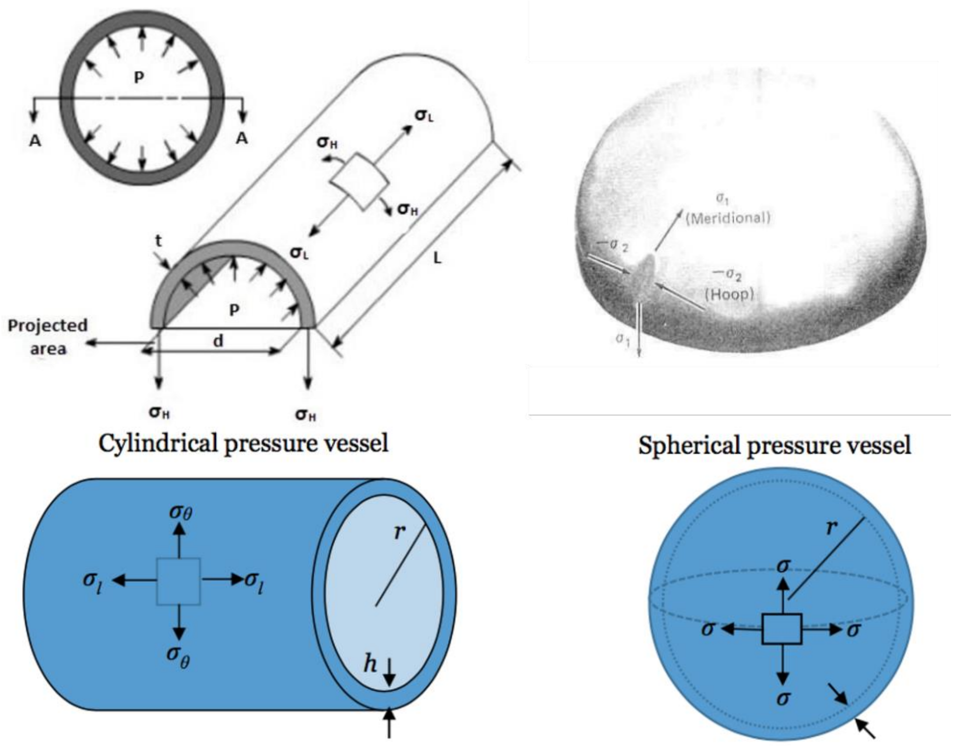

Figure 5: Stresses in Pressure Vessels

[Image Source: (Harvey, 1985; Hazizi & Ghaleeh, 2023)]

2.1.4 Burst Pressure

Burst pressure, within the context of a pressure vessel, refers to the maximum internal pressure the vessel can endure before rupture. This parameter holds immense significance for the safe design and operation of pressure vessels, as surpassing the burst pressure threshold can result in catastrophic failure, leading to the release of contents under high pressure, posing severe risks.

Pressure vessels are intentionally designed with a margin of safety, and the determination of burst pressure is typically undertaken during the vessel’s design and testing phases. Various factors, including material strength, thickness, and vessel geometry, are pivotal in establishing the burst pressure. Engineers and manufacturers ensure that pressure vessels are constructed to withstand pressures significantly higher than the maximum operating pressure to mitigate the risk of potential failures.

The primary formula utilized for determining burst pressure in pressure vessel design is Barlow's equation. Burst pressure depends on both the material's strength and the dimensions of the pressure vessel, including factors such as wall thickness, inside and outside diameter. Temperature variations also play an important role in variation of burst pressure by directly affecting the material's strength. However, in this research, no temperature variation is considered. It's crucial to incorporate a safety factor when calculating the working pressure of pressure vessels. The following analytical equations are generally employed to estimate the burst pressure:

1. Barlow’s equation, 1836

$$P_b = \frac{2St}{D_1} \tag{2.3}$$

2. Turner’s equation, 1910

$$P_b = S ln(\frac{D_o}{D_i}) \tag{2.4}$$

3. Faupel’s equation, 1956

$$P_b = \frac{2}{\sqrt{3}}\sigma_{ys}\left(2 - \frac{\sigma_{ys}}{\sigma_{ult}}\right) ln(\frac{D_o}{D_i}) \tag{2.5}$$

2.1.5 Liquefied Petroleum Gas

Liquified petroleum gas generally is a mixture of hydrocarbons derived from petroleum which are in gaseous state at normal temperature and pressure but may be condensed to the liquid state at normal temperature by applying moderate pressure (NS 380, 2054). LPG mainly consist of one or more of the following gases:

- Propane
- Propylene
- n-butane
- Iso-butane
- Butylene

LPG is a mixture of commercial butane and commercial propane. The boiling points of LPG are very low. Propane and butane have their boiling point at – 42 °C and -0.5 °C respectively at normal atmospheric pressure. LPG when stored inside a vessel is in a mixture of 80% liquid and 20% vapor state. LPG is normally odorless and colorless. At atmospheric pressure and temperature, LPG is a gas which is approximately 2 times heavier than air. The density of the LPG in the liquid state is approximately half of the density of water and ranges from 525 to 580 kg/m^3.

LPG when stored inside a storage vessel or cylinder will exert a vapor pressure corresponding to the temperature of the LPG in the storage vessel. The vapor pressure is dependent on the temperature as well as on the ratio of the mixture of the hydrocarbons.

2.1.6 Liquid Petroleum Gas Cylinders

LPG cylinders are pressure vessels composed of cylindrical shells and hemispherical or ellipsoidal or tori-spherical head ends. Generally, the 14.2 kg LPG cylinder is composed of a single cylindrical shell and is enclosed by two 2:1 ellipsoidal head. The Figure 6 shows the shell and head section of the LPG cylinders.

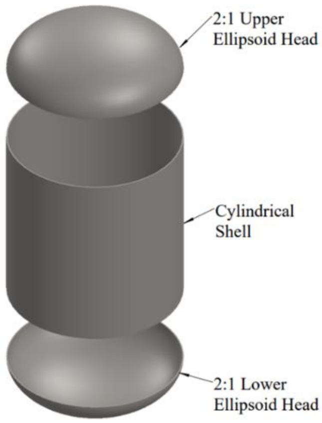

Figure 6: Cylindrical Pressure Vessel Sections

While manufacturing the LPG tank, two symmetrical parts are produced by deep drawing treatment and are joined together by circumferential welding. One symmetrical part is composed of both the ellipsoidal head ends and half the section of the cylindrical shell. The Figure 7 shows the two symmetrical parts before prior to the welding.

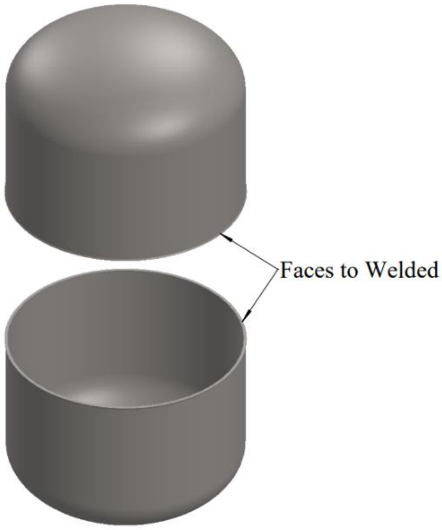

Figure 7: LPG cylinders before welding

2.1.7 Nepal Standards

2.1.7.1 Specifications

The design specification for the LPG cylinders exceeding 5 liter up to 250 liters of water capacity is provided in the NS 369, Specifications of LPG Cylinders – First Amendments, 2053. The section provides a detail design procedure for obtaining the thickness of the cylindrical shell and the ellipsoidal head. The section specifies that the shell thickness shall not be less than 2 mm for cylinders with water capacity up-to and including 13 liters and not less than 2.4 mm for cylinders above 13 liters water capacity (NS 369, 2053). The design criteria for the thickness of the cylindrical shell and the ellipsoidal head as per NS 372, 2067 are given in the .

2.1.7.2 Test Methods for LPG Cylinders

Nepal Standards have described various methods of test for welded low carbon steel cylinders which are intended for the storage and transportation of low-pressure liquefiable gases. The section NS 372, Test Methods for LPG Cylinders, 2067 describes the various test methods that can be used for the LPG cylinders exceeding 5 liter and up to and including 250-liter nominal water capacity. The test included are as follows:

Part 1: Acceptance Test

Part 2: Burst and Volumetric Expansion Test

Part3: Hydrostatic Stretch Test

Part4: Hydrostatic Test

Part5: Pneumatic Leakage Test

Part6: Radiographic Examination

1 **Acceptance Test:** In this acceptance test, one cylinder from a batch of 202 or less is generally selected at random. From the sample cylinder, the following test specimen are cut out:

a) Tensile Test:

i. **Test specimen for parent (P) metal tensile testing:** Two test specimen are cut out from the longitudinal and the transverse direction of the cylindrical portion of the LPG cylinder. Later in the result section the test specimen from the transverse direction will be referred to as PT specimen and that from the longitudinal direction will be referred to as PL specimen.

ii. **Test specimen from welds (W):** Three test specimen are cut out from the circumferential weld region, one for the tensile test, one for the root bend test and the last for the face bend test.

The layout of the test specimen for the acceptance tensile test is given in Figure 8 which is based on NS 372, 2067.

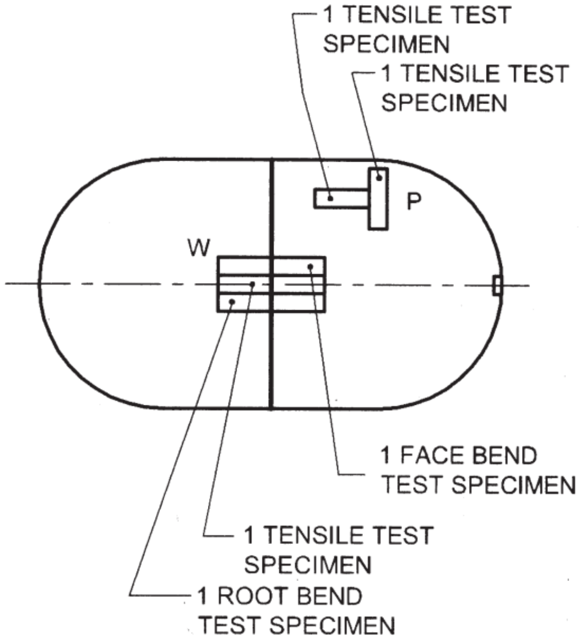

Figure 8: Layout of Test Specimen for Acceptance Test for Two Piece Cylinder
[Image Source: NS 372, Test Methods for LPG Cylinders, 2067, FIG. 1]

b) **Minimum Thickness Test**: A ring is cut from the knuckle portion of the cylinder used for the tensile test. The wall thickness of the ring is measured and should not be less than the calculated wall thickness. Since, during the forming process while manufacturing, the thickness of the cylinder around the knuckle region might get lower than the minimum wall thickness required, this test is important to ensure that the minimum thickness is maintained.

2 Hydrostatic Burst Pressure Test:

A hydrostatic burst pressure test is a pressure test where pressure vessels such as pipelines, LPG cylinders, boilers and tanks are tested for its strength and leaks. The test involves filling of water in the cylinder and pressurizing the cylinder till it bursts. The pressure at which the cylinder burst is known as the burst pressure of the cylinder. This burst pressure must be around 3 times higher than the normal working pressure of the cylinder. As per NS 372, 2067 the following procedures are followed while performing the burst pressure test.

1. One random cylinder sample from each batch of 403 or less is taken and will be subjected to an internal hydrostatic pressure till it burst.
2. The initial original volume of the cylinder before the test and the final volume after the burst will be measured for each sample.
3. Before performing the burst pressure test, the sample cylinder must be subjected to the hydrostatic stretch test and the value of the hydrostatic stretch test pressure for LPG is generally taken as 25 Kgf/cm^2 (NS 372,2067).

A typical arrangement for the hydrostatic burst pressure test is given in the Figure 9.

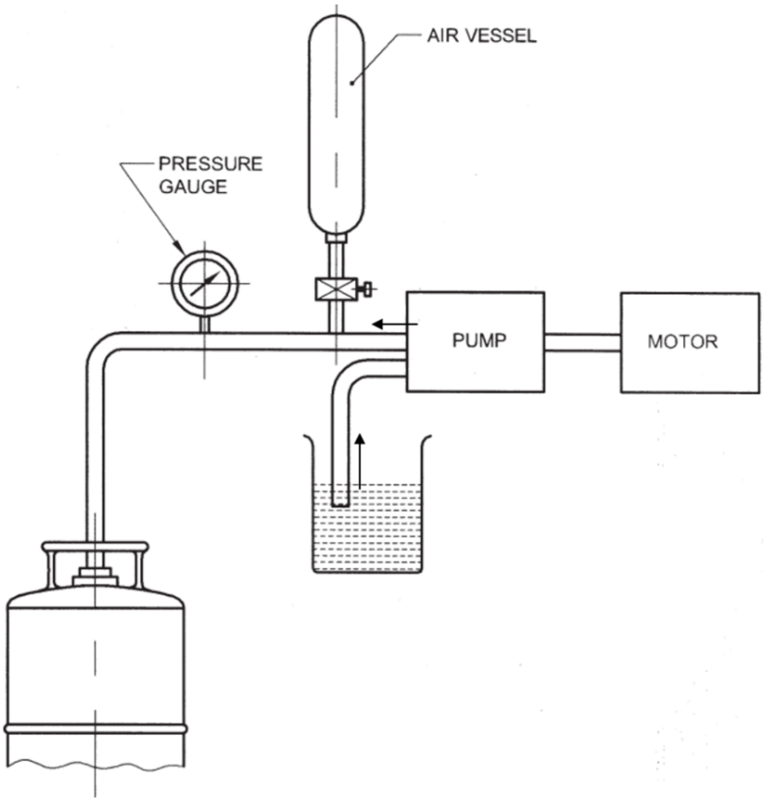

Figure 9: A typical arrangement for the Burst Pressure Test
[Image Source: NS 372, Test Methods for LPG Cylinders, 2067, FIG. 9]

2.1.8 ASME BPVC VIII

ASME BPVC Section VIII has two different divisions where it describes the design and analysis procedures of the pressure vessels. Division 1 can be used for design of pressure vessels with simple geometry configuration. This method of designing pressure vessels using analytical formula are defined as design by rule (DBR) method and for the pressure vessel with complex geometry, the DBR approach will be insufficient and thus another design method is implemented.

Division 2 is used for the pressure vessel with complex geometry and utilizes the design by analysis approach which was not present in the Division 1. Under this division, various analysis (DBA) methods are provided to study the strength and stresses developed within the pressure vessel.

2.1.8.2 Design by Rule (DBR)

The design calculation as per DBA is provided in the .

2.1.8.1 Design by Analysis (DBA)

Three different analysis methods are described under DBA which are as follows:

- Elastic Analysis
- Limit Load Analysis
- Elastic Plastic Analysis

A. Elastic Analysis

In general, stresses can be divided into three classes: primary, secondary, and peak stresses. Primary stresses can further be classified into general membrane stresses, local membrane stresses, and primary bending stresses (Moss & Basic, Pressure Vessel Design Manual, 2013). Thus, there are following types of stresses in summary:

1. Primary Stress, P
    a. General Membrane Stress, P_m
    b. Local Membrane Stress, P_l
    c. Primary Bending Stress, P_b
2. Secondary Stress, Q
    a. Secondary Membrane Stress, Q_m
    b. Secondary Bending Stress, Q_b
3. Peak Stress, Q_f

The description of the stresses is provided as below:

- **Primary Stresses:**

  These are normal or shear stresses which are developed within a structure in response to the external loads or actions. In pressure vessels, the primary stresses are generally due to internal or external pressures. The primary stresses are divided into membrane and bending stresses. It is important to differentiate primary stresses into membrane and bending. The bending stresses are permitted to reach higher stress values than that of a primary general membrane stress. So, primary general membrane stresses are considered more critical than primary bending stresses.

  Primary general membrane stress in pressure vessel is present away from the discontinuities. They are average primary stress across the cross section of the vessel. Primary local membrane stress in general is localized, self-limiting and are produced due to shell and head juncture. A typical example of primary bending stress is represented by the stresses at the center of a flat head.

- **Secondary Stresses:**

  Secondary stresses are normal or shear stresses that develop within a structure as a result of deformation caused by the primary stresses. Likewise primary local membrane stresses, secondary stresses are also self-limiting. In cylindrical pressure vessel, secondary stresses arise due to the geometrical discontinuity at the head and shell juncture. Secondary stresses are generally less significant than primary stresses. Secondary stresses are further classified into two additional classes, membrane and bending.

In general, in a pressure vessel, these all types of stresses are present somehow. Among these stresses, it is necessary to distinguish which class of the stress causes failure of the structure. As primary stresses induce secondary stresses, primary stresses are more critical than secondary stresses. However, within primary stresses, membrane stresses are more critical than bending stresses. These all criteria are summarized in the
As from the, following selection criteria can be done as per ASME Section VIII, Division 2.

- The general primary membrane stresses are compared with the basic allowable stress (either yield or ultimate).
- The local primary membrane stress is compared with the 1.5 times the basic allowable stress.
- The sum of the general primary membrane and the primary bending is compared with the 1.5 times the basic allowable stress.
- The sum of the primary general membrane, primary local membrane and the primary bending stresses are compared with 1.5 times the basic allowable stress.

B. Limit Load Analysis

This material model comprises of two distinct regions, one is the elastic region which is defined up to the limit point and other is the perfectly plastic region which is defined beyond the limit point. Limit load is the maximum load that a structure can safely support. Initially, when the load increases, displacements rise linearly within the elastic range until they hit the yield point. Beyond this yield threshold, the load-displacement relationship becomes nonlinear, with plastic or permanent displacements progressively increasing in proportion to the applied stress. As plasticity spreads throughout the structure, the limit load is reached when the plastic zone expands, resulting in unbounded displacements and structural collapse. At this point, the load-deformation curve flattens, suggesting that the structure can no longer maintain equilibrium under external loads, resulting in irreversible plastic deformation and failure due to loss of equilibrium. According to the ASME code, limit analysis employs an ideal elastic-perfectly plastic material model. Although this idealized approach may appear impractical, most pressure vessel code committees consider it a conservative and useful design model. In this model, the yield stress is set to 1.5 times the allowed stress of the pressure vessel material.

C. Elastic Plastic Analysis

A multi-linear material model, which establishes the linear connection between stress and strain by defining Young's modulus up to the yield point, is used in the study of elastic plastics. Furthermore, for various plastic ranges, matching tangent moduli are established. When compared to linear analysis, elastic plastic material model being non-linear analysis produces better findings.

2.2 Finite Element Method and Software

2.2.1 Finite Element Method

The finite element method (FEM) emerges as a robust numerical technique employed for evaluating the burst pressure of pressure vessels. This method involves dividing the geometry of the pressure vessel into a mesh comprising discrete elements, with the goal of approximating the structural response to internal pressure.

Both the linear and nonlinear material behavior are considered while performing the FEA. The simple constitutive model is the linear elastic model for which the stress and strain are related by Hook’s law given in equation 2.6 for a simple one-dimension case.

$$\sigma = E\varepsilon \qquad (2.6)$$

For three-dimension case, the above equation (2.12) can be written in terms of stress – strain tensor as given by equation 2.7.

$$\begin{Bmatrix} \varepsilon_{11} \\ \varepsilon_{22} \\ \varepsilon_{33} \\ \varepsilon_{12} \\ \varepsilon_{13} \\ \varepsilon_{23} \end{Bmatrix} = \begin{bmatrix} 1/E & -v/E & -v/E & 0 & 0 & 0 \\ -v/E & 1/E & -v/E & 0 & 0 & 0 \\ -v/E & -v/E & 1/E & 0 & 0 & 0 \\ 0 & 0 & 0 & 1/G & 0 & 0 \\ 0 & 0 & 0 & 0 & 1/G & 0 \\ 0 & 0 & 0 & 0 & 0 & 1/G \end{bmatrix} \begin{Bmatrix} \sigma_{11} \\ \sigma_{22} \\ \sigma_{33} \\ \sigma_{12} \\ \sigma_{13} \\ \sigma_{23} \end{Bmatrix} \tag{2.7}$$

For most of the structural problem involving metals such as low carbon steels, if the stresses are below the yield limit, linear elastic material model can be used. However, if the stresses are above the yield limit, i.e., in the plastic region, this model cannot be used and thus elastic-plastic material model must be used for the analysis.

2.2.2 ANSYS

ANSYS is finite element analysis software used predominantly in the field static structural. ANSYS, a widely used finite element analysis (FEA) software, plays a crucial role in the context of pressure vessel simulation, particularly in the domain of static structural analysis. Static structural analysis with ANSYS involves evaluating the mechanical behavior of pressure vessels under various loading conditions, enabling engineers to predict stresses, deformations, and failure modes. Both linear and non-linear models can be setup using the ANSYS. In order to study the plastic failure in ANSYS, limit load and elastic plastic model setup can be used.

CHAPTER THREE: LITERATURE REVIEW

3.1 Reviewed Papers

Literatures on the burst pressure prediction of pipes and cylinders dates back early to the 1800s. The earliest research regarding the burst pressure can be traced back to the Barlow (1836) and Turner (1910). Barlow (1836) in his book has provided a formula to relate the burst pressure that a cylindrical pipe can withstand. The barlow's formula is mostly used in the pipeline industry to design the safe internal pressure limit. Turner (1910) in his paper provided a formula to calculate the burst pressure of a thick cylinders. Both the Barlow's and Turner's formula are the most importatnt and the earliest formula that relates the burst pressure of the cylindrical pipes and pressure vessels.

Bhattarai (2023) in his study utilized Abaqus simulation to analyze stress and deformation in domestic LPG cylinders. Experimental burst pressures ranged from 14 MPa to 19 MPa, with an average of 15.5 MPa. Hoop stress values varied from 866.6 MPa to 1176.1 MPa. Von Mises Stress ranged from 750.4976 MPa to 1018.53 MPa. The analysis aims to enhance safety and reliability of LPG cylinders for domestic use. Learning from failures is crucial for improving engineering practices.

In a study done by Abdussalam (2006), it was found that FEA of thin-walled aerosols cans was as effective as experiments and can be used extensively to model the manufacturing processes of the cans. Elastic and elastic-plastic FEA was conducted to study the phenomenon of the yielding and plastic collapse due to internal pressure. The study found that the FEA predictions and the experimental data are in close aggreement with each other. However, the author recommends using FEA over the traditional experiment methods because of the repeatability and rapid re-analysis capacity.

Magar, Basnet, and Ghimire (2023), performed a FEA using DEAL.II, a powerful opensource FEA tool to assess the structural and safety assessment of medical oxygen cylinders.

Accurate burst pressure prediction is crucial for any component design and safety, typically achieved through analytical and empirical methods. Some of the studies involves a comparative estimation of burst pressure using the existing analytical failure models of a cylinders and is compared with FEA. Wang, Zheng, Sang, & Krakauer

(2021) in their paper evaluated the burst pressures of a large dimeter to thickness ratio thin-walled cylinders using both experiments and FEA. The burst pressures were evaluated using the existing failure models and was compared with each other. Christopher, Sarma, Potti, Rao, and Sankarnarayansamy (2002) in their paper performs a comparative study on estimating the failure pressure of cylindrical vessels using existing test data, theories and various procedures. Oh, Race, Oterkus, and Chang (2020) in their paper, developed a new methodology for predicting burst pressure in flawless API 5L X grade pipelines using finite element analysis with a bilinear material model based on the tangent modulus approach. Nonlinear finite element parametric study was conducted, resulting in an empirical formula for estimating burst pressure. The proposed formula showed excellent agreement with burst test results, indicating its accuracy for API 5L X grade pipelines. Zhu, Wiersma, Johnson, & Sindelar (2023) in their paper, explored the burst pressure solution for the thick-walled cylinders using the Zhu-Leis solution and compared with the two most known Von-Mises and Tresca solution criteria.

Brabin, Christopher, and Rao (2011) in their paper performed burst experiment on different steel cylindrical vessels and compared with the existing predictive analytical equations. It was found that the Faupel's bursting pressure formula is the most simple and reliable while predicting the burst strenght of the thin-walled cylindrical steel vessels.

Kisioglu (2009) in his paper studied the burst pressure and volume expansion of a toroidal LPG fuel tank using both the experiment and FEA approaches. Hydrostatic burst tests were performed for the experiments and 2D nonlinear plane models were developed using axisymmetric boundary conditions for FEA. The study found a bursting pressure of 8.77 and 8.56 MPa using the FEA and experiments.

Dharmarao (2015) focuses on determining stress variations in thick-walled pressure vessels using both the analytical and FEA methods. For the analytical methods, the paper employs Lame's and Clavarino's equations while for the FEA methods, ABAQUS has been employed. Results from both the analytical and FEA based methods are in close agreement with each other.

Rangari, Zode, and Mehar (2012) performed FEA of an existing LPG cylinder to verify its burst pressure. Low carbon steel was used as a material for the research. The cylinder was subjected to increasing internal pressure while doing the FEA using axisymmetrical boundary conditions. They calculated maximum shear stress, equivalent shear stress at critical areas using both FEA and analytical theoretical formulas and concluded the verification of the FEA ANSYS prediction with theoretical solution.

Wang, Yao, Li, Sang, and Krakauer (2017) in their paper examines the buckling behavior of the externally-pressurized, thin-walled, torispherical bottom head of residential electric water heater tanks using both experimental and finite element analysis (FEA) methods. The study found that the geometry imperfections have a more significant impact on buckling pressure than the contact imperfections, providing valuable insights for the design and manufacture of water heater tanks.

Palanivelu and Prasad (2017) in their paper performed an axisymmetic FEA of the ellipsoidal type pressure vessel and determined the stress distribution and failure location. The analytical results and the FEA results are compared with each other. The study found that for axisymmetrical vessels, the critical failure point is near the equator of the head.

Aksoley, Ozcelik, and Bican (2007) in their paper have analyzed the LPG tanks as a pressure vessels. They have performed experimental and FEM analysis by varying the internal pressure values. The study was performed for LPG tanks drawn with two different sheet thickness values of 3mm and 2.8mm. The experimental results and the FEM analysis are in coherance with each other and the paper concludes that LPG tanks can be produced in compliance with the standards even when the sheet thickness is lowered to 2.8mm from 3mm resulting in lower production cost.

Mohamed (2018) in his study considered linear elastic material model to perform FEA of a thin-walled cylinder with flat ends. The hoop and longitudinal stresses are analyzed. The results from the FEA model is compared with the theory from the solid mechanics. The paper found a good hoop and axial stress distribution across the cylinder wall thickness and concludes that it is unwise to use the flat end plates in pressured cylinders.

OZKAN, OZHAN and GENC (2019) has published their paper in which a detailed methodology for the design and analysis of a pressure vessel with hemispherical head has been presented. The burst pressure is calculated using all the design by analysis approaches in addition with design by rule appraoch. Out of all the approaches, the design by rule appraoch is the most conservative for which the burst pressure obtained is 3.814 MPa and the obtained burst pressure from the elastic plastic analysis is 4.94 MPa, which is the largest of all the other approaches.

Bhatia and Mohammad (2019) in their study proposes to determine the burst pressure of LPG tanks using FEM. The LPG tank has a wall thickness of 2.8 mm for which the FEM results are computed. The FEM results are in close aggrement of the experimental data. The FEM burst pressure simulated was 115 bar and the average experimental burst pressure obtained was 120 bar.

Yin, Su, and He (2019) examines an industrial oxygen cylinder using ANSYS Workbench to perform a FEA. The study determines stress values and distribution using the equivalent stress linearization techniques to optimize the structure of the container.

Kaptan and Kisioglu (2007) performed a series of experiments and computer simulation to study the burst pressure and its location. In the study, 2D axisymmetric geometry has been used. The burst pressure were obtained for three different tank capacity keeping the nominal thickness of the 2.5 mm constant. The burst pressure obtained from experimental results are 9.07, 8.52, and 7.72 MPa. Similarly, 9.68, 8.57, and 7.94 MPa were obtained from the FEA modeling for the tank capacity of 35, 60, and 85 Liter.

Fadel and Yahya (2021) conducted experimental burst tests on LPG cylinders, determining burst pressures and failure locations through hydrostatic testing, and examining permanent volume expansions resulting from internal pressure.

Hazizi and Ghaleeh (2023) focuses on designing a vertical pressure vessel for safely storing 10 m^3 of pressurized LPG according to ASME code standards. Using Autodesk Inventor Professional and Inventor Nastran for modeling and finite element analysis, the research found that increasing shell thickness improved safety by reducing displacement and increasing the factor of safety. The manway and shell experienced the highest stresses, prompting structural adjustments to enhance vessel safety.

Wadkar et al. (2015) in their paper presented a methodology for the design and analysis of the pressure vessel using the Mechanical APDL ANSYS. The paper discusses the design codes and rules as per the ASME BPVC Division 1. The analytical results are compared with the simulation results from the ANSYS for both the head and shell section.

Macwan and Hu (2011) in their paper aimed to assess the pressure and mechanical behavior of pressurized thick-walled cylinders subjected to high stress. The study evaluates hoop strain and hoop stress on both the inner and outer surface. The experimental results obtained are compared with theoretical Lame's solution and FEA results. All the three results are in close agreement with each others.

Jegatheesan and Zakaria (2018) focuses on designing pressure vessel according to three different standard codes available; ASME BPVC Section VIII Division 1, PD 5500, and EN 13445. In the study PVElite is used to design a storage tank and study the stresses. Out of these three standards, the ASME code demonstrates superior performance compared to British and European Standards.

Yahya, Daas, Alboum, and Khalile (2018) in their paper designed a vertical pressure vessel using the ASME BPVC Section VIII Division 1. This paper addresses the hazards associated with incorrectly designed pressure vessels used for storing hazardous fluids. A FEA was also done to validate the ASME stress results in SolidWorks Software and found that the design ensures compliance with the ASME codes and engineering standards.

A new methodology DBA-L has been proposed by Li, Huang, Yang, and Yang (2017) that circumvent the stress categorization by extending the elastic stress analysis approach given in the ASME BPVC Section VIII Division II based on the lower bound limit load theory.

Zhou, Patel, Wang, Jin, and Li (2021) in their paper introduces a methodology to optimize the material using an intergrated approach. Both the ANSYS and MATLAB are used to study the stress and optimize the material while complying with the ASME BPVC Section VIII Division II. Elastic analysis has been emplyed in order to optimize the shell and the flange thickness by keeping the maximum linearized memrane and membrane plus bending stress way below the allowable code limits.

Ugochukwu, Oluwole, and Odunfa (2018) used finite element method to investigate the displacements, deflections and the von-mises stresses within the cylindrical LPG pressure tank. In doing so, the thickness of the plate, the operating pressure and the ambient conditions are varied. ANSYS was employed for the mesh generation and the analysis. The results showed an inverse relationship between the shell thickness and displacement, deflection, and Von-Mises stress under different LPG pressures. Also, a linear relationship was observed between the factor of safety and the shell thickness.

Wibawa (2020) investigates the von-mises stress and factor of safety in the thin-walled cylinders for the rocket motor case by varying the wall thickness and the internal pressure. FEA is done using the ANSYS software and it shows that the value of the von-mises stress decreases with the increasing wall thickness and increases with the increasing internal pressure. The results of the FEA was compared with the analytical calculation for maximum hoop and axial stress and showed that the percentage errors to be within 6%.

Patil and Jadhav (2017) in their paper reviewed various studies on the failure and optimization of the pressure vessels, focusing mainly on the stress concentration at the junctions, excessive deformations from the improper support, reinforcement and end connections.

Collectively, these studies offer valuable insights into the diverse methods and considerations employed in analyzing and predicting the burst pressure and failure behavior of pressure vessels, providing a nuanced understanding of their structural performance and safety implications.

3.2 Research Gap

Despite the existence of multiple formulas designed to forecast the burst pressure of pressure vessels, a significant gap persists between these theoretical predictions and actual experimental findings. The review of past literatures on design and analysis of pressure vessels, LPG cylinders reveals that most of the existing research is based on foreign context, which may not be applicable to Nepal. Also, significant research gap exists in the understanding of LPG cylinder failure mechanisms and safety practices in Nepal. The unavailability of data such as burst strength, material properties, and the limited use of modern FEA tools in the design and analysis are the major fields the research tries to address.

CHAPTER FOUR: RESEARCH METHODOLOGY

This chapter describes the methodology used in the research work. The thesis involved the modeling, testing and simulating a 14.2 Kg LPG cylindrical type pressure vessel, commonly used as a cooking application to assess its strength, safety and associated risk. A flowchart of the methodology used during the thesis work is provided in the Figure 10.

The research work began with the study of the literature and the past reviews on the topic of pressure vessels and LPG cylinders. After the completion of the literature review, a site visit was made for performing and collecting the experimental data. During this phase, the tensile test and hydrostatic burst pressure test was performed. Also, during the site visit, the detail dimension of the 14.2 Kg LPG cylinder was also collected. And then, both the 3D and 2D CAD model of the LPG cylinder was created using the SOLIDWORKS software. The CAD model was then imported into the FEA software ANSYS for a detailed finite element analysis. Since the LPG cylinder is axisymmetric about the longitudinal axis, a 2D axisymmetric FEA was done using the Static Structural Workbench. The 2D axisymmetric model of the LPG cylinder was meshed and boundary conditions such as internal pressure loading, fixed displacement, frictionless support, symmetry was applied for the simulation. The simulations were run using three different material model such as elastic material model, elastic perfectly plastic material model, and elastic plastic material model. The results from the simulations were compared and verified with the experimental data and the theoretical calculations using the shell theory approach. The results were then post processed for the documentation and the presentation. In addition, the literature review was conducted throughout the thesis duration on various related topics.

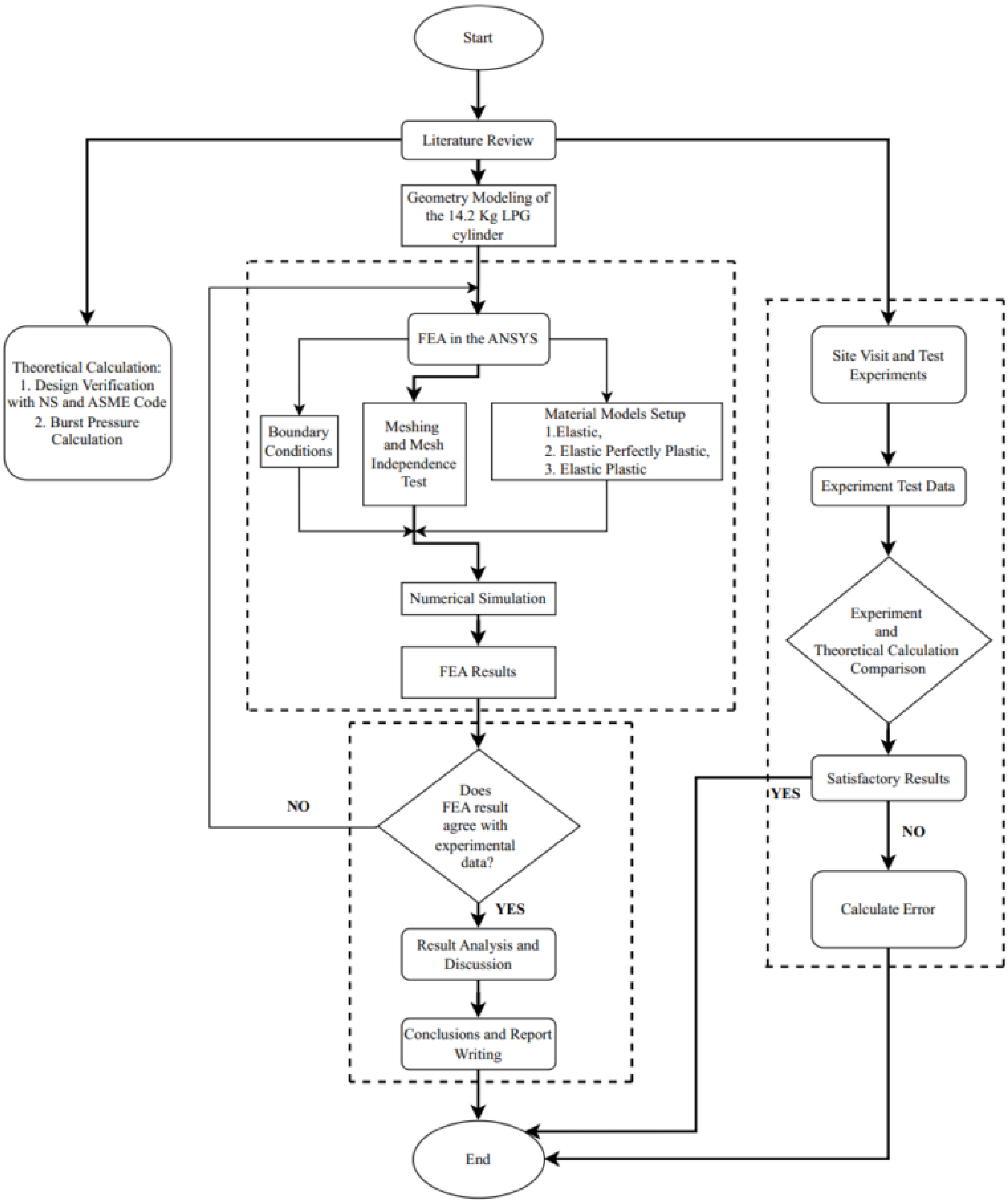

Figure 10: Methodology of research

The different stages shown in the research methodology flowchart is discussed below in their separate section.

4.1 Literature Review

A comprehensive literature review was conducted throughout the thesis duration to ensuring that standard paths were chosen. The literature review involved evaluating and studying the existing research, past literatures and theories, allowing for a comparison of different stages undertaken with those of the standard established methods. The method of review ensured that the research was thorough, comprehensive, and followed industry best practices. During this phase, literatures on the pressure vessels, LPG cylinders, ASME BPVC and Nepal Standards, and FEA as per DBA were reviewed and studied thoroughly for the successful completion of the research.

4.2 Site Visits and Test Experiments

After stating the research problem, a site visit was planned for performing the experiments such as tensile test and hydrostatic burst pressure test. These two tests must be performed as per Nepal Standards in order to ensure the safety of the LPG cylinders. Experimental test for the tensile test and hydrostatic burst pressure test were conducted at Arrowtech Private Limited at Birgunj, Nepal on 15th March at 11 am to 2 pm. As per Aksoley et al. (2008), the use of large number of experimental data would results in less error between FEM simulation and experimental burst pressure values. So, nine sets of LPG cylinder samples were taken for each tensile and burst pressure test in this research. All the test is done as per stated by the NS 372, 2067.

4.2.1 Tensile Test

A uniaxial tensile test was performed in order to determine the mechanical properties of the metal. Low carbon steel metal is generally used a material for the manufacturing of the LPG cylinders. The test specimen was collected as per described in the section 2.1.7.2 under Chapter Two. Three test samples were considered for the tensile test from Nine different LPG cylinder sample. So, a total of 27 test specimen were tested for the tensile test in order to determine the average yield strength and the ultimate tensile strength of the steel metal. The Figure 11 shows the tensile test specimen before and after the fracture with a gage length of 50 mm marked down.

b

a

Figure 11: Tensile Test Specimen: (a) Before, (b) After the fracture

The results obtained from the tensile test is presented under the Tensile Strength Test under Experimental Results section of the Chapter 5.

4.2.2 Minimum Thickness Test

Following the tensile test, minimum thickness test was also performed for Nine different LPG cylinder samples. In this test, a ring of section was cut down from the knuckle of the LPG cylinder in order to measure the minimum thickness around the region.

4.2.3 Hydrostatic Burst Pressure Test

A hydrostatic burst pressure test for Nine different LPG cylinder samples was done in order to obtain the experimental burst pressure. As per NS 372, 2067, the following procedures were followed while carrying out the burst pressure test:

1. The initial weight of the LPG cylinder was measured in order to the obtain the tare weight of the cylinder.
2. The LPG cylinder was filled with water and the total weight of the setup was again measured in order to obtain the water capacity of the cylinder.
3. Now, a hydrostatic stretch test was performed. For this hydrostatic stretch test, the pressure for was taken as 25 Kgf/cm^2 (2.45 MPa). The cylinder samples that withstand the hydrostatic stretch test were sent for the hydrostatic burst pressure test.
4. Now for the hydrostatic burst pressure test, the pressure was increased from 2.45 MPa till the LPG cylinder ruptures and explodes. Just before the bursting of the LPG cylinder, the weight of the expanded LPG cylinder with water is measured in order to determine the volume expansion of the cylinder.

The Figure 12 shows the LPG cylinder sample before and after the hydrostatic burst pressure test.

a b

Figure 12: LPG Cylinder Sample: (a) Before, (b) After hydrostatic burst pressure test

The results obtained from the minimum thickness test and the hydrostatic burst pressure test is presented under the Hydrostatic Burst Pressure Test of CHAPTER FIVE: RESULTS AND DISCUSSION.

4.3 Theoretical Calculation

This section covers two topics as follows:

4.3.1 LPG Cylinder Design Verification as per NS, ASME and Shell Theory

The chosen 14.2 Kg LPG cylinder as per Nepal Standards have an average wall thickness of about 2.61 mm, inner diameter of about 314.4 mm and 2:1 ellipsoidal formed head. The LPG cylinder model can be divided into two sections: one is open cylindrical shell section and other is the 2:1 ellipsoidal head section.

Here, in this section, the design of the chosen LPG cylinder is checked with three different codes and standards.

1. Nepal Standards
2. Shell Theory Concepts
3. ASME BPVC VIII

Considering the wall thickness, material properties such as yield strength for the material chosen, the minimum permissible internal pressure is calculated. The results of this section are provided in the section 5.2.1 Design Verification using NS, Shell Theory and ASME Code for which the formulas are presented in the .

4.3.2 Burst Pressure Prediction

For an internal pressure near the experimental burst pressure, stresses such as hoop and axial stress are calculated as per solid mechanics. These stress values are compared with the yield and ultimate strength of the material to determine the theoretical burst pressure for the 14.2 Kg LPG cylinder. The literatures on the different stresses present in the pressure vessel are provided in the section Stresses in the Pressure Vessel under Chapter 2.

4.4 Geometric Modeling of the LPG cylinder

A 3D CAD model of the 14.2 Kg LPG cylinder was prepared. The design specification of the commercial 14.2 Kg LPG cylinder is provided in the Table 1.

Table 1: Design Specification of 14.2 Kg LPG Cylinder
[Source: NS 369, 2053; NS 367, 2053]

LPG Cylinder Details	
Certifications	Nepal Standards
Material	Hot Rolled Steel
Density of the Steel	Around 7850 Kg/m³
Minimum Yield Strength	240 MPa
Tensile Strength	350 – 450 MPa
Design Temperature	-40° C to 60°C
Water Capacity	33.3 Liter
LPG Capacity	14.2 Kg ± 50 gram
Tare Weight of the cylinder	15.3 - 15.5 Kg
Total Weight of the cylinder	29.5 - 29.7 Kg
Overall-height of LPG Cylinder	625 mm
Height up-to the Bung Top	488 mm
Outer Diameter	320 mm
Inner Diameter	314.4 mm
Working Pressure	1.65 MPa
Test Pressure	2.45 MPa
Burst Pressure	Around 8 – 9 MPa
Minimum Thickness of the Cylinder	2.4 mm
Length of Cylindrical Portion	330.5 mm
Type of Dome	Ellipsoidal 2:1

The specification tabulated above is sourced from both the Nepal and Indian Standards. Hot rolled steel plate is used to draw the cylinder whose density is around 7850 Kg/m³. The empty weight of the LPG cylinder is around 15.3 to 15.5 Kg. The working pressure inside the cylinder is around 1.65 MPa and the test pressure is around 2.45 MPa.

Generally, the minimum thickness of the cylinder wall is 2.4 mm for which the burst pressure must be around 2.5 times the test pressure.

4.4.1 Modeling of the LPG Cylinder

The 3D model of the LPG cylinder considered for the analysis in this research is prepared using the CAD software SolidWorks. The Figure 13 shows the general drawing used to model the LPG cylinder. The top handle and bottom base are not shown in the figure. The LPG cylinder is a 2:1 Ellipsoidal head type cylindrical pressure vessel for which the inner diameter of the cylinder is 314.4 mm and the overall height of the cylinder shell is about 493 mm. The detail view C shows the thickness of the cylinder considered which is 2.61 mm.

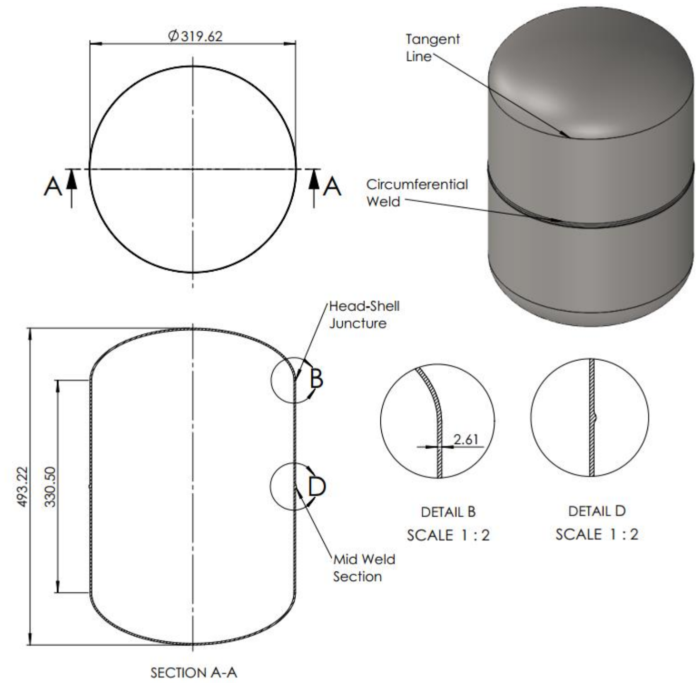

Figure 13: Drawing of the LPG Cylinder Model

4.4.2 Material Properties of the LPG Cylinder

The properties of the steel used to manufacture the cylinders must conform to Nepal Standards 367. The tensile strength, yield strength and percent elongation must be as per the Table 2 provided by the NS 367, 2053.

Table 2: Material Properties for the Structural Steel According to NS 367, 2053

Tensile Strength, MPa	Yield Strength, MPa (Minimum)	Percentage Elongation, % (Minimum)
350 - 450	240	25

The tensile strength, yield strength of the material must be greater than the material properties provided in the Table 2. Tensile test of the steel plate is performed for 9 different specimens. The details of the tensile test are presented in the chapter 5.

4.5 FEA in the ANSYS

In this section, all the procedures undertaken while performing the FEA of the LPG cylinder in ANSYS is presented. First of all, the 3D model of the cylinder is meshed in the ANSYS Modeler and then materials and physics is setup. The boundary conditions associated with the simulation are applied. The details of the process are presented in the sections below.

4.5.1 Mesh Creation and Mesh Independence Test

1. Mesh Creation

Since, the LPG cylinder is axisymmetric about both the X and Y axis. Only the quarter of the vessel is subjected to the simulation. The quarter model of the vessel is then meshed and a 2D axisymmetric simulation is then performed. A 0.5 mm of body sizing was used for the quarter model of the vessel results in total of 3564 number of elements. The reason to select this specific number of elements is provided in mesh independence test section. Quadrilateral type element is used while meshing the computational domain as shown in the Figure 14.

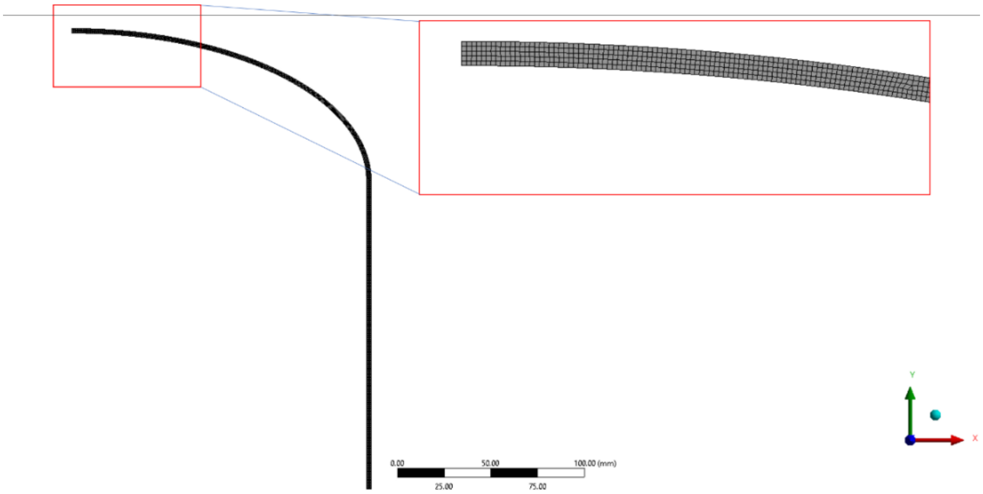

Figure 14: Mesh Showing the LPG Section

The axisymmetric model when revolved along the y-axis and mirrored through XZ plane will result the full-scale model of the pressure vessel as shown in the Figure 15.The Figure 15 shows the mesh created for the full 3D LPG cylinder for visualization purposes only.

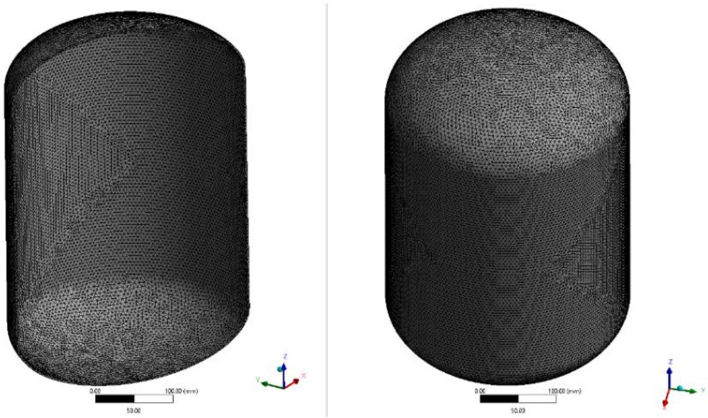

Figure 15: Mesh Showing the LPG Shell Domain (Whole)

2. Mesh Independence Test

A mesh independence study is conducted to ensure that simulation results remain stable as mesh resolution is refined. This means the simulation outcomes do not significantly change with varying mesh sizes. During the study, the element size is progressively increased, and the accuracy of the resulting solutions is evaluated. Typically, a finer mesh involves larger elements, which increases computational time, whereas a coarser mesh uses fewer elements, reducing computational time. Performing a mesh independence study is crucial to achieving an optimal balance between the accuracy of the solution and computational efficiency.

In this study, ANSYS static structural simulation is ran for various mesh sizes. The internal pressure is kept at 1 MPa and boundary conditions kept is frictionless support and the results of the mesh independence test is provided in the section 5.3.1 Mesh Independence Test Results of the section 5.3 Numerical Simulation Results.

4.5.2 Material Model and Analysis Setup

ANSYS Mechanical is used to perform the numerical simulation of the LPG cylinder. Linear and non – linear material model is prepared for the simulation. Three different analysis model is prepared as follows:

1. Elastic Analysis
2. Limit – Load (Elastic Perfectly Plastic) Analysis
3. Elastic Plastic Analysis

The Figure 16 shows the difference between these analysis methods:

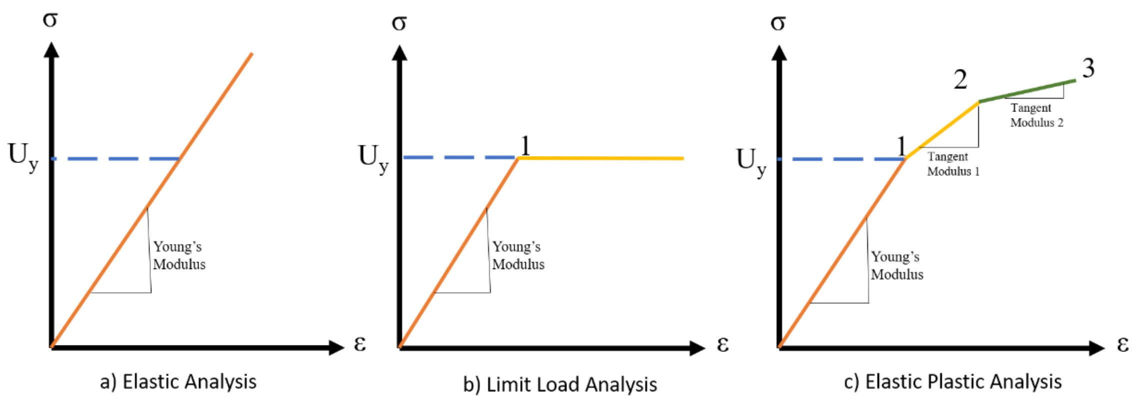

Figure 16: Stress-Strain curve for various analysis Type

1 Elastic Analysis:

In elastic analysis, a linear material model is prepared. The stress and strain are linearly related and the young's modulus and the poison's ratio is defined. The yield and ultimate strength values are not used. Here, linear material model is applied.

2 Limit Load Analysis:

In limit-load analysis, a linear material model is prepared up-to the yield point. Beyond the yield point, the strain increases infinitely without any increase in the stress. Bilinear material model is applied where young's modulus, poison's ration and the yield strength are defined. Here, elastic-perfectly plastic material models are utilized for which the stress-strain curve is shown in the Figure 16b. In this analysis method, the strain hardening behavior of the material is neglected. Yield strength of 283.88 MPa and Tangent Modulus of 0 MPa is applied as shown in the Figure 17.

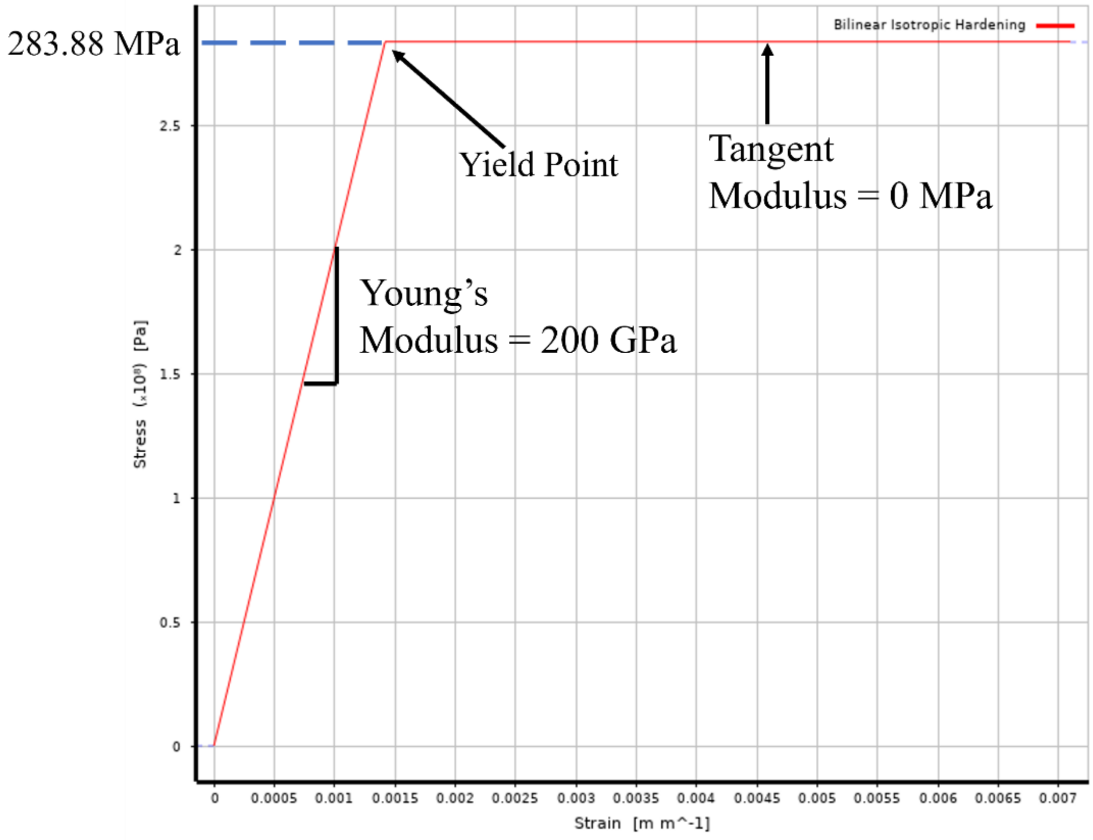

Figure 17: Bilinear Material Model for the Limit Load Analysis

3 Elastic Plastic Analysis:

In elastic plastic analysis, multi-linear material model is applied where young's modulus is defined up-to yield point which defines the linear relationship between stress and strain. Also, corresponding tangent moduli is defined for different plastic range. Elastic plastic analysis is a non-linear analysis which gives more accurate results as compared to linear analysis. The material has an engineering yield strength of 283.88 MPa and engineering ultimate tensile strength of 421.045 MPa with a strain of 36.61 % at fracture. The engineering stress and strain values are converted into the true stress and strain values

$$\sigma_{true} = \sigma_{eng.} \times (1 + \varepsilon_{eng.}) \qquad (4.1)$$

$$\varepsilon_{true} = \ln (1 + \varepsilon_{eng.}) \qquad (4.2)$$

For elastic-plastic analysis, strain is provided in terms of plastic strain. As we know, the total strain is a sum of elastic strain and plastic strain. The following equation can be used to obtain the plastic strain using the total and elastic strain.

$$\varepsilon_{plastic} = \varepsilon_{total} - \varepsilon_{elastic} \tag{4.3}$$

where,

$$\varepsilon_{elastic} = \frac{\sigma_{true}}{E} \tag{4.4}$$

E = Young’s Modulus

The true stress-strain curve for the material using this approach is presented in the Figure 18 where the x-axis represents the true plastic strain and y-axis represents the true stress in MPa.

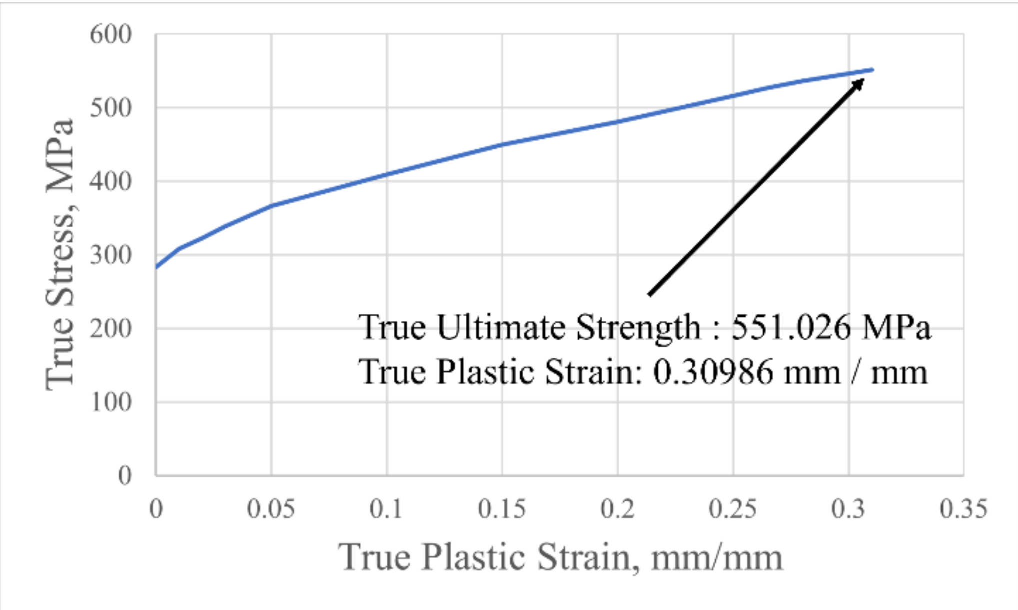

Figure 18: Stress-Strain Relation for Elastic-Plastic Analysis

4.5.3 Boundary Conditions and Physics Setup

Boundary conditions are crucial in determining how a system behaves at its edges, playing a vital role in solving mathematical models like partial differential equations (PDEs) within a computational domain. Properly defining these conditions is essential for simulations to yield meaningful and accurate results, mirroring the behavior of the real-world system. Boundary conditions serve as parameters that guide computational processes, ensuring the reliability and validity of the simulation outcomes.

1 Displacement Boundary Condition

LPG tanks are symmetrical about both the longitudinal axis represented by the y-axis and along the XZ plane as shown in the Figure 19 .So, we can employ 2D axisymmetric analysis for which the axis of symmetry is Y– axis. Here, the lower face is represented by the letter B in the Figure 19 and is given a displacement boundary condition. The displacement of the face B is restricted in the y-direction and is free to move in XZ plane trying to model the symmetry of the LPG tanks along XZ plane. The internal surface represented by the line A is given a boundary condition of pressure loading.

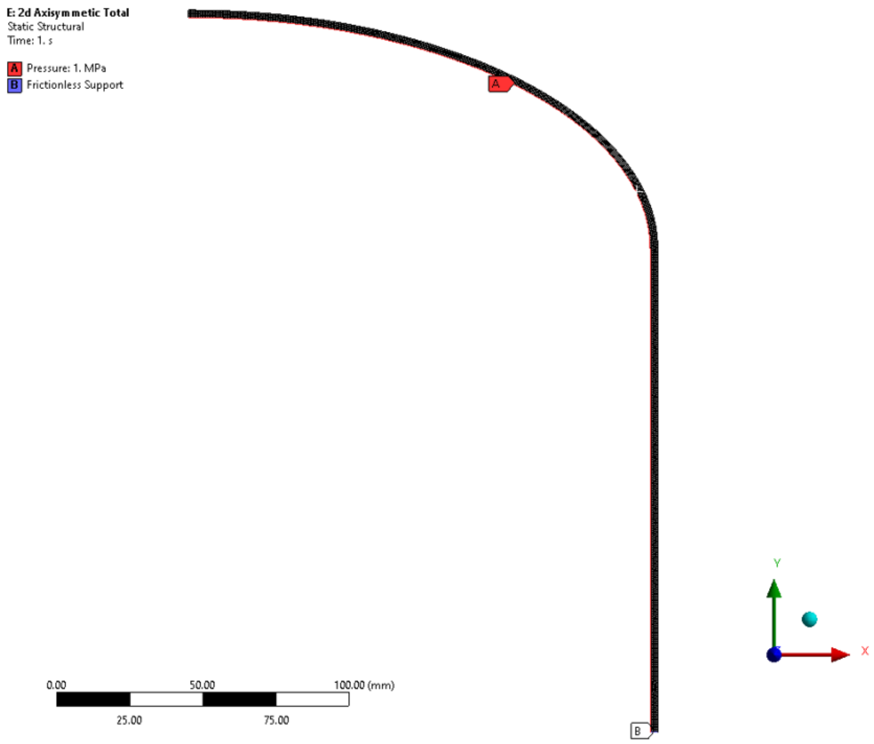

Figure 19: Boundary Conditions

2 Internal Pressure Loading

Various values of internal pressure are given as an input to the simulation software ANSYS. The internal surface of the LPG cylinder is set as a pressure boundary condition for which the simulation is run. The Figure 20 shows the internal loading used in the simulation of the LPG cylinder.

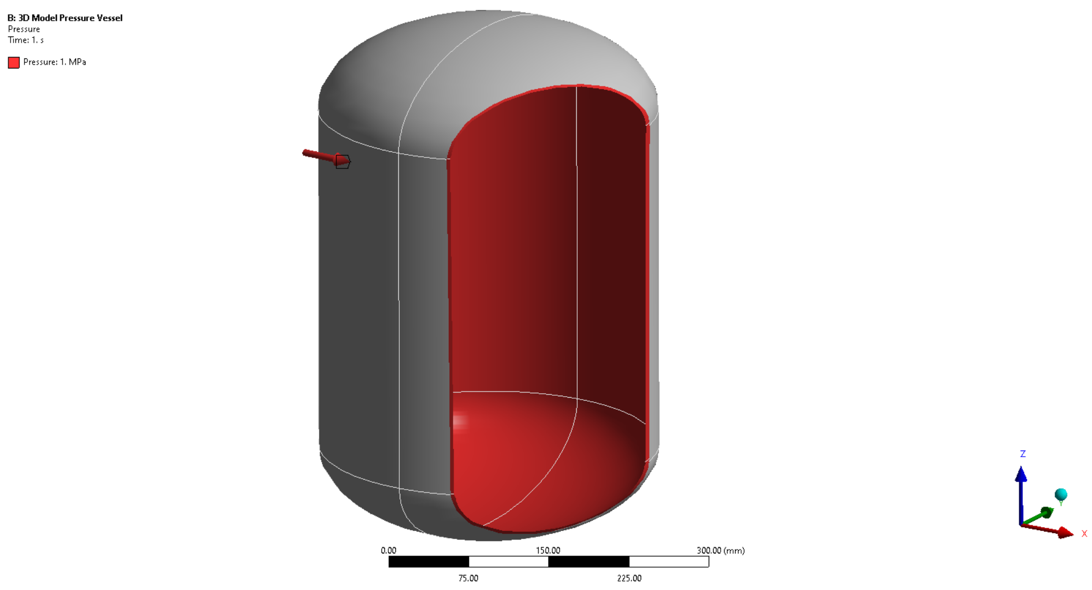

Figure 20: Internal Pressure Loading Conditions

4.5.4 Numerical Simulation

An axisymmetric numerical simulation as described in the ASME BPVC Section VIII Division 2 Part 5 is done following the above-mentioned procedures for which the burst pressure is determined and is compared with the analytical and the experimental burst pressure.

4.6 Result Validation, Discussion and Analysis

After the successful completion of the numerical simulation, the simulation results are compared with the experimental data. Also, the theoretical solution and experimental data are also compared. The detail analysis of the results is presented in the Chapter 5 of the thesis report. Here in this section, the experimental results are discussed followed by the analytical theoretical calculation and the FEA predictions. Different stresses such as equivalent von-mises, hoop and axial are described under the numerical simulation.

4.7 Conclusions and Recommendations

The conclusions obtained from the research work is presented in this section following the recommendations for the further work.

CHAPTER FIVE: RESULTS AND DISCUSSION

In this chapter, the results from the experiment and simulation are presented and discussed.

5.1 Experimental Result

5.1.1 Tensile Strength Test

From this test, the overall yield strength, ultimate tensile strength obtained from the tensile test are 283.879 MPa and 421.045 MPa respectively. These results are used to predict the failure analysis of the LPG cylinders. The Table 3 shows the experimental data obtained from the tensile test.

Table 3: Result from Tensile Test (Yield and Tensile Strength)

Test Sample	**Test Specimen PT**		**Test Specimen PL**		**Test Specimen W**
	Yield Strength (Kgf/mm^2)	**Ultimate Strength (Kgf/mm^2)**	**Yield Strength (Kgf/mm^2)**	**Ultimate Strength (Kgf/mm^2)**	**Ultimate Strength (Kgf/mm^2)**
1	29.93	41.08	28.26	38.86	49.41
2	28.57	39.18	29.09	39.56	49.23
3	27.31	40.68	30.67	39.54	49.82
4	28.28	39.46	28.98	39.13	49.23
5	27.58	39.72	28.9	39.85	49.45
6	30.87	39.19	29.09	38.98	50.29
7	28.95	40.27	30.14	41.49	49.24
8	27.5	38.05	29.35	37.77	49.52
9	28	38.62	29.41	40.58	50.64
Average (Kgf/mm^2)	28.55	39.58	29.32	39.53	49.65
Average (MPa)	280.12	388.31	287.64	387.78	487.04

The Table 3 shows that the ultimate strength for the specimen W is more than both the specimen PT and specimen PL. Since, the stresses near the discontinuity due to weld will be much higher than the normal membrane stresses, the ultimate strength of the cylinder at this weld region should be higher than other regions. Also, the percentage elongation of the test specimen is also recorded and is tabulated in the Table 4.

Table 4: Result from Tensile Test (Percentage Elongation)

Test Sample	Percentage Elongation	
	Test Specimen PT	Test Specimen PL
1	39	36
2	36	34
3	35	36
4	39	36
5	36	38
6	33	34
7	42	38
8	36	36
9	39	36
Average	37.22%	36%
	36.61%	

The Table 4 shows that the average percentage elongation for the test specimen is 36.61.

5.1.2 Hydrostatic Burst Pressure Test

LPG cylinders are taken at random from each batch and are subjected to an internal hydrostatic pressure till it bursts. The initial original volume and the volume after the test of the cylinder are then measured. Total of nine specimens of the cylinders were subjected to hydrostatic burst pressure test. The average burst pressure obtained is about 8.72 MPA. The Table 5 shows the experimental data obtained from the hydrostatic pressure burst test.

Table 5: Result from the Hydrostatic Pressure Burst Test

S.N.	Min. Thickness (mm)	Empty Weight of Cylinder (Kg)	Weight of Cylinder with Water (Kg)	Water Capacity (Kg)	Burst Pressure (Kgf/cm2)	Crack Location
1	2.63	15.23	48.7	33.47	90.00	LVF
2	2.62	15.2	48.7	33.5	80.00	SVF
3	2.59	15.4	49	33.6	90.00	LVF
4	2.57	15.3	48.8	33.5	90.00	LVF
5	2.65	15.2	48.6	33.4	90.00	LVF
6	2.63	15	48.5	33.5	100.00	LVF
7	2.59	15.2	48.9	33.7	90.00	LVF
8	2.61	15.3	48.9	33.6	80.00	LVF
9	2.6	15.2	48.8	33.6	90.00	SVF

Avg	2.61	15.23	48.77	33.54	88.89	
Avg (MPa)					8.72	

From the Table 5, it is seen that the average internal pressure that will result in bursting of the LPG tanks is around 8.72 MPa. Long vertical fracture around weld region is seen in maximum of the test cases. The tare weight, i.e., the empty weight of the cylinder is around 15.23 kg whereas the water capacity of the cylinders is around 33.54 kg. The total weight of the cylinder with water is around 48.77 kg.

5.1.3 Experiment Result compliance with NS 367, 2053

The yield strength, ultimate strength, and percent elongation of the material obtained from the experiment is checked with the criteria as provided in the NS 367, 2053. The Table 6 shows the results compliance of the experimental data with the criteria given in the NS 367, 2053.Table 6: Experimental Data Compliance with NS 367, 2053

Table 6: Experimental Data Compliance with NS 367, 2053

Material Properties	NS 367, 2053 Criteria	Experimental Results
Yield Strength, MPa	240 (Minimum)	283.879 MPa
Ultimate Strength, MPa	350-450	421.045 MPa
Percent Elongation, %	25 (Minimum)	36.67 %

The Table 6 shows that the obtained experiment values are within the criteria set by NS 367, 2053. Thus, the experiment data shows that the structural steel used to manufacture the 14.2 LPG cylinder confirms with the NS 367, 2053.

5.2 Analytical Results

5.2.1 Design Verification using NS, Shell Theory and ASME Code

The minimum permissible internal pressure is obtained for the yielding of the material. The yield strength is chosen as the allowable stress limit. The obtained yield strength of the material from the experiment is 283.879 MPa. The wall thickness is 2.61 mm.

1. **As per Shell Theory:**

   Here, the wall thickness of the LPG cylinder is only 2.61 mm and the inner radius is 157.2 mm. The r/t ratio for this cylinder is 60.229. Thus, the LPG cylinder can be approximated as a thin wall pressure vessel. Since the LPG cylinder consists of cylindrical shell and 2:1 ellipsoidal head. The minimum burst pressure is calculated for both the cylindrical and ellipsoidal portion and the lower value between them is chosen.

a. Cylindrical Portion:

For the cylindrical portion, the maximum stress obtained is hoop stress which is double the longitudinal stress. The formula relating the burst pressure, wall thickness, inner radius and the hoop stress is given as:

$$\sigma = \frac{P_b r}{t} \tag{5.1}$$

Using the formula 3.1, keeping the hoop stress equal to the allowable yield strength of about 240 MPa, we get the wall thickness as,

$$\text{Or,} \quad P_b = \frac{\sigma * t}{\mathrm{r}}$$

$$\text{Or,} \quad P_b = \frac{283.879 \times 10^6 \times 2.61}{157.2}$$

$$\therefore \quad P_b = 4.7132\ MPa$$

Thus, for the cylindrical portion of the LPG cylinder, minimum internal pressure of about 3.9847 MPa is obtained.

b. Ellipsoidal Head:

For the ellipsoidal head portion, the hoop (circumferential) and the longitudinal (meridional) stress are not same as in the case of hemispherical head. Both the hoop and the longitudinal stress varies from maximum at the crown and gradually decreases at the equator (Harvey, 1985). Also, the a/b ratio plays important role in the type of stress developed near the equator region. The Figure 21: Plot of stresses in ellipsoidal with variation in ratio a/b shows the longitudinal and the hoop stress developed for the various a/b ratio:

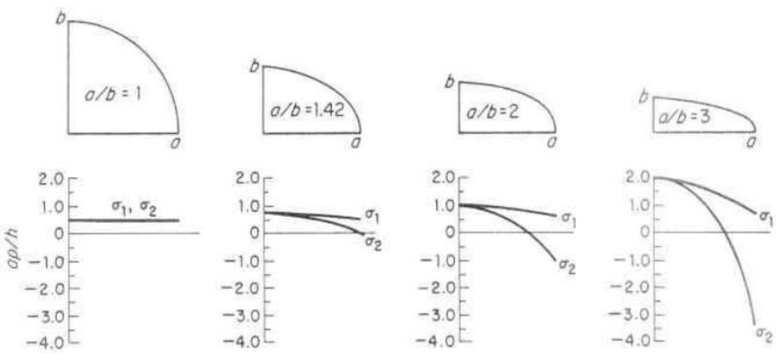

Figure 21: Plot of stresses in ellipsoidal with variation in ratio a/b
[source: (Harvey, 1985)]

Since, the head in the LPG considered is 2:1 ellipsoidal, near the equator region, compressive stresses are formed. Near the crown region, both the longitudinal and the hoop stresses are same. Near the shell and head juncture, both the stresses decrease gradually. The hoop stress for ellipsoids with a/b ratio greater than 1.42 becomes compressive as seen from the Figure 41. So, for the burst pressure calculation, we can use the formula at the maximum stress position which is at the crown region. Also, at the equator, for the compressive hoop stress we can obtain the corresponding burst pressure. The analytical formula for the cases is taken from the Harvey, 1985.

i. **At the crown region:**

Both the hoop and the longitudinal stress are equal and is given as:

$$\sigma = \frac{P_b \times a^2}{2 \times b \times t} \tag{5.2}$$

Which gives the burst pressure of 4.7132 MPa.

ii. **At the equator region:**

The hoop stress at the equator is given as:

$$\sigma = \frac{P_b \times a}{t}\left(1 - \frac{a^2}{2 \times b^2}\right) \tag{5.3}$$

Which gives the internal pressure of 4.7132 MPa which is same as that of the cylindrical case. Here, the allowable yield stress is taken as compressive.

Thus, as per shell theory, the minimum burst pressure obtained for the LPG cylinder is 4.7132 MPa. Since the working pressure inside the LPG cylinder is only about 1.65 MPa, the 14.2 Kg LPG cylinder is safe.

2. **As per Nepal Standards:**

Literatures relating the Nepal Standards are provided in the chapter section 2. NS 369 provides a comprehensive design methodology for the calculation of the LPG cylinder wall thickness. It provides a separate calculation procedure for the cylindrical shell and the 2:1 ellipsoidal head portion.

i. **Calculation of the cylindrical shell thickness:**

1.

$$t = \frac{P_h D_o}{200 \times 0.8 J R_e + P_h} \qquad 5.4$$

2. $$t = \frac{P_h D_i}{200 \times 0.8 J R_e - P_h} \quad 5.5$$

3. $$t = 0.136 \times \sqrt{D_o} \quad 5.6$$

The greater values between B.4, B.5, and B.6 should be selected for the cylindrical shell thickness. Using formula 1 and 2, the corresponding minimum burst pressure obtained considering the wall thickness of 2.61 is presented in the Table 18:

Table 18: Minimum Permissible Internal Pressure according to NS

Formula	P_h in kgf/cm^2	P_h in MPa
1.	38.1229	3.7385
2.	38.1229	3.7385

Which gives the minimum pressure of about 3.7385 MPa. Thus, according to NS, the LPG cylinder is safe for the test pressure of 25.30 kgf/cm^2 or 2.48 MPa. Also, using the formula 3 for the wall thickness, we get the minimum wall thickness, t = 2.43 mm. Since, the chosen wall thickness of 2.61 mm is greater than 2.43 mm, it is seen that the chosen wall thickness is conservative.

ii. Calculation of the ellipsoidal head thickness:

1. $$t = \frac{P_h D_o}{200 \times 0.8 J R_e + P_h} \times \frac{K(0.65 + 0.1K)}{4} \quad 5.7$$

Which gives the minimum internal pressure of 36.302 kgf/cm^2 or 3.56 MPa. This value of burst pressure is greater than that of the cylindrical portion. Thus, the design is safe for a hydrostatic test pressure of 25.30 kgf/cm^2.

3. As per ASME BPVC:

The ASME codes (ASME, ASME Boiler and Pressure Vessel Code VIII - Div 1, 2023) provide fundamental guidelines for designing the pressure vessel shells and heads for various design criteria. For the thickness chosen, the permissible internal pressure or burst pressure can be found using the following equations:

1. $$Pc_{cylinder} = \frac{S \times E \times t}{R + 0.6 \times t} \quad (5.8)$$

$$\text{or, } P = \frac{283.879 \times 1 \times 2.61}{157.2 + 0.6 \times 2.61}$$

$$\therefore P = 4.6667 \text{ MPa}$$

2. $$P_{\text{Ellipsoidal}} = \frac{2 \times S \times E \times t}{D + 0.2 \times t} \tag{5.9}$$

$$\text{or, } P = \frac{2 \times 283.879 \times 1 \times 2.61}{314.4 + 0.2 \times 2.61}$$

$$\therefore P = 4.705 \text{ MPa}$$

For the cylinder wall thickness of 2.61 mm, 283.879 MPa of maximum allowable stress value, joint efficiency of 1, the allowable internal pressure for the cylindrical shell section is found to be around 4.6667 MPa and for the ellipsoidal head section to be around 4.705 MPa. So, as per ASME design codes, the pressure vessel is able to withstand around 4.6667 MPa for which both the shell and head section are safe. Beyond this 4.667 MPa, plastic deformation starts to occur and at certain value of internal pressure, the vessel will burst, this pressure is known as burst pressure.

The minimum permissible internal pressure for which the 14.2 Kg LPG cylinder will be safe is 3.56 MPa as given in the Table 7. Out of the three approach, Nepal Standards is the safest as it limits the minimum permissible internal pressure at 3.56 MPa, i.e., a minimum internal pressure of 3.56 MPa can be applied for which the yielding of the 14.2 Kg LPG cylinder does not occur. Since, the working and test pressure as provided in NS 367, 2053 is around 1.65 and 2.45 MPa, the LPG cylinder design is safe. Here, the yield strength of the material is considered as the allowable stress limit, i.e., the bursting of the LPG cylinder will not occur at this pressure but rather at higher values of the internal pressure.

Table 7: Table for minimum permissible internal pressure using codes and standards

	As per Shell Theory (MPa)	As per Nepal Standards (MPa)	As per ASME BPVC (MPa)
Cylindrical Shell	4.7132	3.7385	4.6667
Ellipsoidal Head	4.7132	3.56	4.705

5.2.2 Burst Pressure Prediction

The membrane stresses such as hoop stress and axial stress is computed analytically considering the LPG as a thin-walled pressure vessel. The Where, t = 2.61 mm, r = 157.2 mm and P is varied from 1 to 15 MPa as shown in the Table 8.

Table 8 shows the analytical primary membrane hoop and axial stress computed at the cylindrical portion of the LPG for an internal pressure ranging from the 1 to 15 MPa. The formula used to compute the hoop and axial stress are as follows:

1. Hoop Stress, $\sigma_{H,\,C} = \frac{P \times r}{t}$ (5.10)
2. Axial Stress, $\sigma_{A,\,C} = \frac{P \times r}{2 \times t}$ (5.11)

Where, t = 2.61 mm, r = 157.2 mm and P is varied from 1 to 15 MPa as shown in the Table 8.

Table 8: Analytical Solutions

S.N.	Internal Pressure (MPa)	Analytical Hoop Stress (MPa)	Analytical Axial Stress (MPa)
1	1	60	30
2	2	121	60
3	3	181	91
4	4	241	121
5	4.7	283.6207	141.81
6	5	302	151
7	6	362	181
8	6.5	392	196
9	6.98	421.2069	210.60
10	7	422	211
11	7.5	453	226
12	8	483	241
13	8.5	513	256
14	9	543	272
15	9.5	573	287
16	10	603	302
17	10.5	634	317
18	11	664	332
19	12	724	362
20	13	784	392
21	14	845	422

22	15	905	453

The Table shows that the hoop stress equals the uniaxial ultimate tensile strength at an internal pressure of 6.98 MPa.

5.3 Numerical Simulation Results

Before performing the numerical simulation in the ANSYS, a mesh independence test was carried out, the results of the test are present in the Mesh Independence Test section below.

5.3.1 Mesh Independence Test Results

The Table 9 summarizes results of the mesh convergence test:

Table 9: Mesh Convergence Test

S.N.	Element Number	Hoop Stress	Axial Stress	Equivalent Stress
1	476	63.505409	31.256552	55.862453
2	1048	63.505970	31.256550	55.863421
3	2378	63.506168	31.256550	55.863761
4	3564	63.506256	31.256550	55.863916

The Table 9 shows a mesh convergence test for an internal pressure of 1 MPa. The element used are quadrilateral. The Table shows the maximum hoop, axial, and equivalent stress developed along the thickness of the pressure vessel with increasing number of element size in the mesh. The Figure 22 plots the graph showing the variation of these stresses with corresponding element size in the mesh.

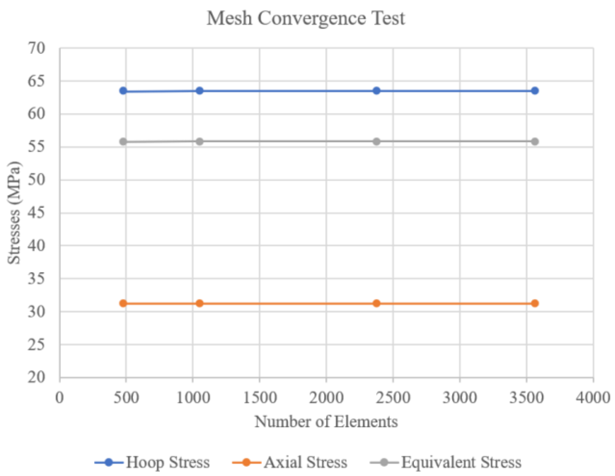

Figure 22: Mesh Convergence Plot

The Figure 22 shows that with increase in the number of the element size from 476 to 3564, the axial stress changes from 31.256552 to 31.256550 MPa which is below 1% change. In the case of hoop and equivalent stress, the values vary with the change in number of elements. The hoop stress changes from 63.506168 to 63.506256 MPa when the number of element changes from 2378 to 3564 and the equivalent stress changes from 55.863761 to 55.863916 MPa which are also below 1% change. Thus, 4th configuration is selected to discretize the computational domain.

After the successful creation of the mesh and the completion of the physics setup and boundary conditions, an elastic axisymmetric numerical simulation of the LPG cylinder has been performed. The results of the numerical simulation are described below. The stress in the Table 10 is recorded for a path 1-2 along the thickness of the cylindrical shell as shown in the Figure 23.

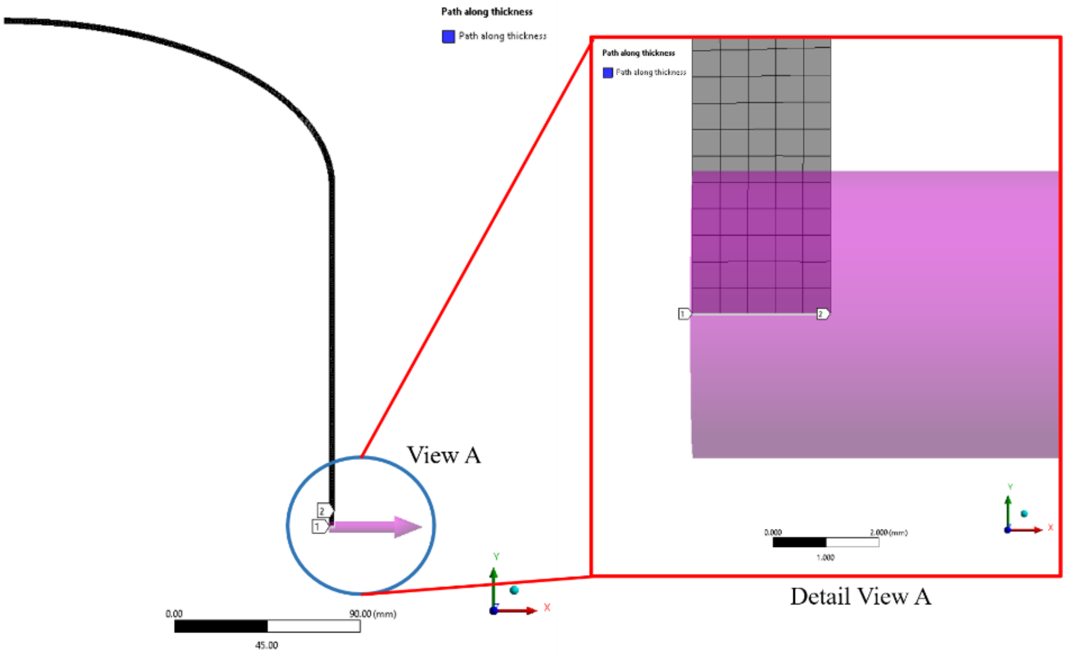

Figure 23: Path through the thickness

The internal pressure is varied from 1 MPa to 15 MPa as shown in the table. The Table 10 shows the hoop stress, axial stress and equivalent von – mises stress.

Table 10: Various Stress component for varying internal pressure - Simulation

S.N.	Internal Pressure (MPa)	Hoop Max. (MPa)	Axial Max. (MPa)	Equivalent Max. (MPa)
1	1	61	30	54
2	2	122	60	107
3	3	183	90	161
4	4	243	120	214
5	5	304	150	268

6	6	365	180	321
7	6.5	396	195	348
8	7	426	210	375
9	7.5	456	224	402
10	8	487	239	429
11	8.5	517	254	455
12	9	548	269	482
13	9.5	578	284	509
14	10	609	299	536
15	10.5	639	314	562
16	11	669	329	589
17	12	730	359	643
18	13	791	389	696
19	14	852	419	750
20	15	913	449	803

From the Table 10, it is seen that as the value of the internal pressure increases, all of the three-stress component gets increases. The equivalent stress becomes greater than 283 MPa which is the yield strength of the structural steel at an internal pressure of around 5.28 MPa and it exceeds 420 MPa which is the ultimate tensile strength of the structural steel at an internal pressure of around 7.833 MPa.

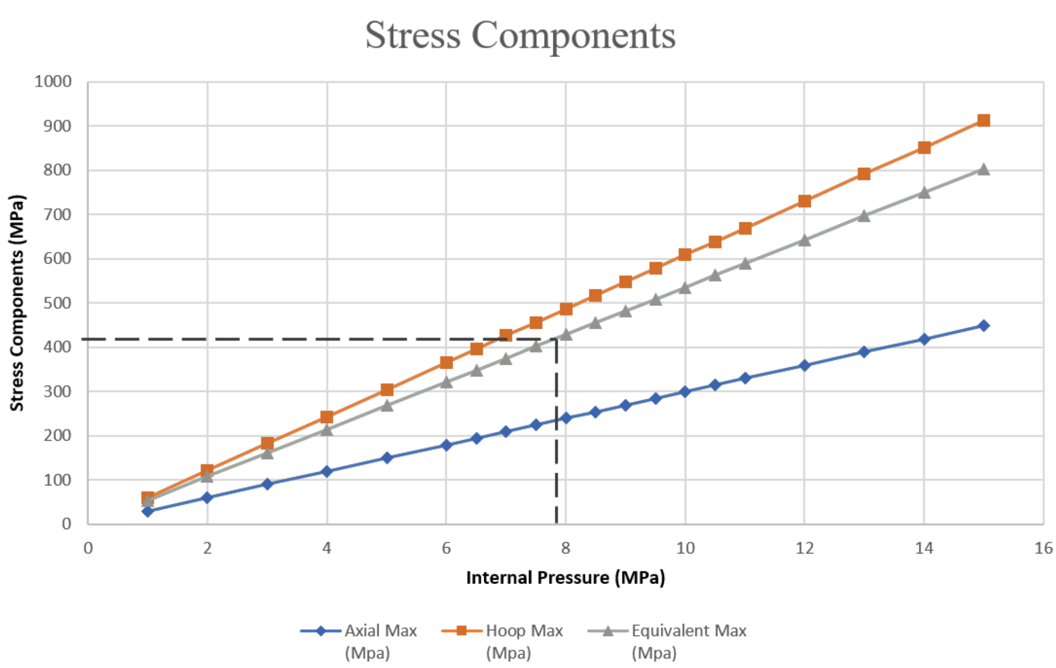

Figure 24: Stress Components with internal pressure over thickness

The Figure 24 shows the plot of equivalent stress, hoop stress and axial stress developed for various values of the internal pressure. The x- axis shows the values of the internal pressure in MPa whereas the y – axis shows the corresponding stress values. The plot shows that with increase in the internal pressure, all the three stresses; equivalent, hoop, and axial stresses increases linearly.

In the above numerical simulation, the stress values are calculated at the cylindrical portion and is compared with the ultimate strength of the metal. This is somehow a conservative and simple method for detecting the failure of the LPG cylinder. In the design by analysis approach by ASME in BPVC section VIII, Division 2, Part 5 has provided failure criteria for protection against plastic collapse of the pressure vessel.

5.3.2 Elastic Analysis Method

Stresses are computed using an elastic analysis which are then classified into categories, and limited to allowable values that have been conservatively established such that a plastic collapse will not occur. An internal pressure load is applied and linear, elastic, and isotropic material properties are utilized for the method. The young's modulus of 200 GPa and poison's ration of 0.3 is utilized. The elastic analysis method neglects the nonlinear geometric and material effects. The stress developed can be greater than both the yield strength and the ultimate tensile strength of the material.

For the elastic stress analysis method, an internal pressure equal to the 7.833 MPa, which is the burst pressure obtained previously is utilized. The Figure 25 shows the plot of equivalent stress for this internal pressure.

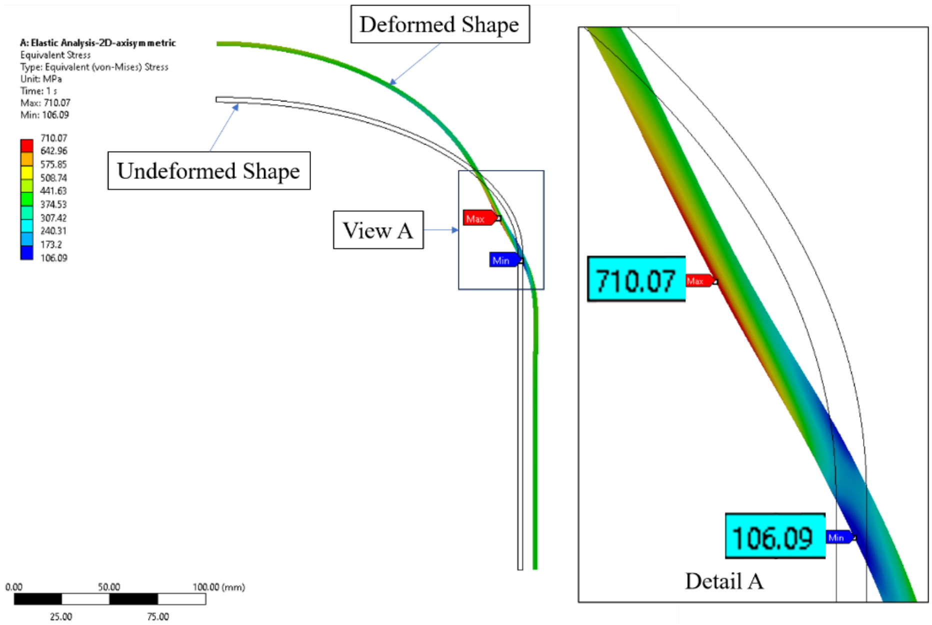

Figure 25: Equivalent Stress for Internal Pressure of 7.833 MPa

The Figure 25 shows that the equivalent stress varies from a minimum of 106.09 to maximum of 710.07 MPa for an internal pressure of 7.833 MPa. The undeformed shape is shown in the wireframe whereas the deformed shape is represented by the color contour. The Figure shows that the maximum equivalent stress is near the head and shell juncture. The variation of the equivalent stress along the longitudinal axis of the cylinder is plotted in the Figure 26.

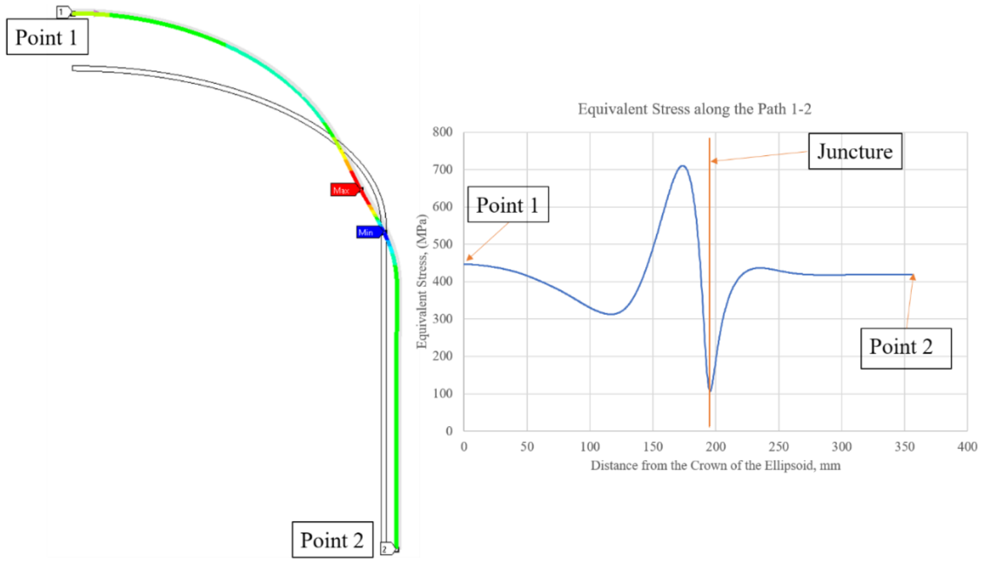

Figure 26: Variation of Equivalent Stress along the Path

The equivalent stress at the crown of the cylinder is 446.36 MPa which then decreases as shown in the Figure. Two peaks can be seen near the head and shell juncture (equator region). The maximum equivalent stress shows about 710 MPa which is at the juncture between the head and the shell and this maximum value of the stress is due to the geometrical discontinuity. This stress value is much higher than the ultimate tensile strength which is not possible for any material. Obviously, the stress values are not true and is not a suitable choice for the selection of the failure criteria.

In the elastic stress analysis, ASME proposes a stress linearization technique which categorizes the elastic stresses present in the structure. The Stresses are categorized into primary general, primary local, primary bending and peak stresses. Primary general stresses are stresses away from any discontinuity while local membrane stresses are present near the local discontinuity. These stresses are then compared with the following limits shown in the Table 11.

Table 11: Stress Categorization and its Limit

Stress Category	Limit	Remarks
Primary General Membrane	S	U_y or U_T
Primary Local Membrane	1.5 × S	S_{PL}
Primary Local plus Bending	1.5 × S	S_{PL}

In order to categorize the elastic stress, a stress linearization needs to be done. The stress linearization of equivalent stress along any line will categorize the equivalent stress into primary membrane, bending and peak stresses. The line at which stress linearization is performed is called stress classification line (SCL) and the location of the SCL defines whether the primary membrane stress is general or local. So, for this four SCL are created as shown in the Figure 27.

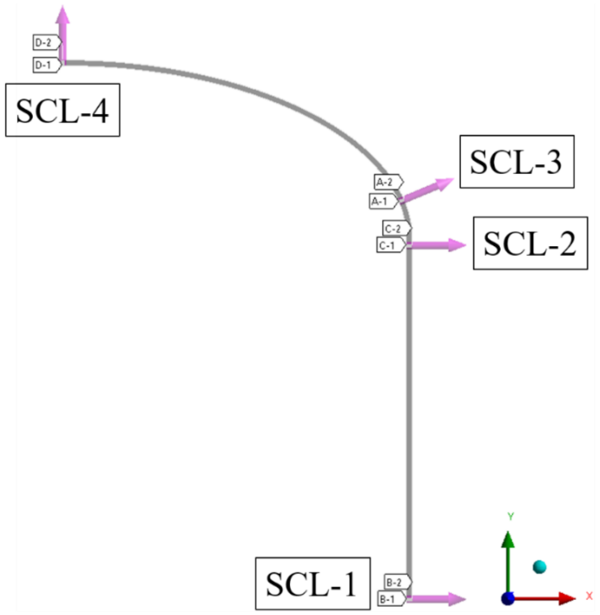

Figure 27: Stress Classification Lines

The SCL-1 and SCL-4 are away from the discontinuity. Thus, the primary membrane stresses given by the linearization is categorized as general stress whereas the SCL-2 and SCL-3 are near the discontinuity region. Thus, the primary membrane stresses given is categorized as local membrane stress. The Table 12 shows the value of the stresses for all of the four SCLs.

Table 12: Elastic Stress Analysis Results

Stress	Membrane equivalent stress			Membrane plus bending equivalent stress			Remarks
SCL	Category	Limit	Stress Value [MPa]	Category	Limit	Stress Value [MPa]	
SCL-1	P_m	S	411.95	$P_m + P_b$	SPL	418.74	Acceptable
SCL-2	P_L	SPL	207.45	$P_L + P_b$	SPL	288.46	Acceptable
SCL-3	P_L	SPL	471.95	$P_L + P_b$	SPL	703.88	Not Acceptable
SCL-4	P_m	S	471.07	$P_m + P_b$	SPL	495.06	Not Acceptable
Allowable Stress Limits		S = 421.05 MPa		Check Criteria	Primary General is checked with S		
		SPL = 1.5 × S			Primary Local is checked with SPL		
		SPS = 1.5 × S			Membrane Plus Bending is checked with SPL		
S = Allowable Stress Value			SPL = Allowable Primary Local			SPS = Allowable Primary Secondary	

So, using the elastic stress analysis approach for an internal pressure of 7.833 MPa, the design is not acceptable. In order to determine or predict the maximum allowable internal pressure (burst pressure), a series of simulation is run by varying the internal pressure from 5 MPa to 10 MPa with a step of 0.25 MPa and for each internal pressure, the corresponding equivalent stresses are categorized using the above approach and is compared with the corresponding stress limit. The Table 13 provides a detail stress categorization along the four SCL and is checked with the allowable stress limit as per ASME BPVC, Division 2, Part 5, Failure against plastic collapse, elastic stress analysis.

Table 13:Elastic Stress Analysis Burst Pressure Analysis

	SCL								
	SCL Number	**SCL-1**		**SCL-2**		**SCL-3**		**SCL-4**	
	SCL Definition	**Away from Discontinuity (Cylindrical Shell Mid Plane)**		**End of Cylindrical Shell**		**Head and Shell Juncture**		**Away From Discontinuity (At the Crown)**	
	Stress Category	Primary General	Membrane plus Bending	Primary Local	Membrane plus Bending	Primary Local	Membrane plus Bending	Primary General	Membrane plus Bending
Internal Pressure [MPa]	**5.00**	262.96	267.29	132.42	82.55	301.26	449.31	300.69	285.03
	5.25	276.11	280.66	139.04	86.67	316.32	471.77	315.73	299.28
	5.50	289.25	294.02	145.66	90.80	331.38	494.24	330.76	313.53

	5.75	302.40	307.39	152.29	94.93	346.45	516.70	345.80	327.79
	6.00	315.55	320.75	158.91	99.06	361.51	539.17	360.83	342.04
	6.25	328.70	334.12	165.53	103.18	376.57	561.63	375.87	356.29
	6.50	341.85	347.48	172.15	107.31	391.63	584.10	390.90	370.54
	6.75	354.99	360.85	178.77	111.44	406.70	606.56	405.94	384.79
	7.00	368.14	374.21	185.39	115.57	421.76	629.03	420.97	399.04
	7.25	381.29	387.58	192.01	119.69	436.82	651.50	436.01	413.30
	7.50	394.44	400.94	198.63	123.82	451.89	673.96	451.04	427.55
	7.75	407.59	414.30	205.25	127.95	466.95	696.43	466.07	441.80
	8.00	420.73	427.67	211.87	132.07	482.01	718.89	481.11	456.05
	8.25	433.88	441.03	218.50	136.20	497.07	741.36	496.14	470.30
	8.50	447.03	454.40	225.12	140.33	512.14	763.82	511.18	484.55
	8.75	460.18	467.76	231.74	144.46	527.20	786.29	526.21	498.81
	9.00	473.33	481.13	238.36	148.58	542.26	808.75	541.25	513.06
	9.25	486.47	494.49	244.98	152.71	557.33	831.22	556.28	527.31
	9.50	499.62	507.86	251.60	156.84	572.39	853.68	571.32	541.56
	9.75	512.77	521.22	258.22	160.97	587.45	876.15	586.35	555.81
	10.00	525.92	534.59	264.84	165.09	602.51	898.61	601.39	570.06
Allowable Limit		S	SPL	SPL	SPL	SPL	SPL	S	SPL
		421.05	631.58	631.58	631.58	631.58	631.58	421.05	631.58

The Table 13 shows the values of the equivalent stress that are categorized using stress linearization. The allowable stress limit is considered to be the ultimate tensile strength of the material which is 421.05 MPa. From the table, it is shown that the maximum allowable internal pressure obtained is in between 7.25 to 7.5 MPa. So, further simulation can be done with lower step size. The elastic stress analysis is further carried out starting from 7 MPa to 8 MPa with steps in-between and stress are checked for allowable limit as described above. The Figure 28 shows the above results.

	SCL								
	SCL Number	SCL-1		SCL-2		SCL-3		SCL-4	
	SCL Definition	Away from Discontinuity (Cylindrical Shell Mid Plane)		End of Cylindrical Shell		Head and Shell Juncture		Away From Discontinuity (At the Crown)	
	Stress Category	Primary General	Membrane plus Bending	Primary Local	Membrane plus Bending	Primary Local	Membrane plus Bending	Primary General	Membrane plus Bending
Internal Pressure [MPa]	7.00	368.14	374.21	185.39	115.57	421.76	629.03	420.97	399.04
	7.0010	368.1951	374.2640	185.4169	115.5820	421.8205	629.1197	421.0311	399.1013
	7.0014	**368.2161**	**374.2853**	**185.4275**	**115.5886**	**421.8446**	**629.1556**	**421.0551**	**399.1241**
	7.0018	368.2372	374.3067	185.4381	115.5952	421.8687	629.1915	421.0792	399.1469
	7.002	368.25	374.32	185.44	115.60	421.88	629.21	421.09	399.16
	7.003	368.30	374.37	185.47	115.62	421.94	629.30	421.15	399.22
	7.004	368.35	374.42	185.50	115.63	422.00	629.39	421.21	399.27
	7.005	368.41	374.48	185.52	115.65	422.06	629.48	421.27	399.33
	7.006	368.46	374.53	185.55	115.66	422.12	629.57	421.33	399.39
	7.007	368.51	374.58	185.58	115.68	422.18	629.66	421.39	399.44
	7.008	368.56	374.64	185.60	115.70	422.24	629.75	421.45	399.50
	7.009	368.62	374.69	185.63	115.71	422.30	629.84	421.51	399.56
	7.010	368.67	374.75	185.66	115.73	422.36	629.93	421.57	399.61
	7.020	369.19	375.28	185.92	115.90	422.97	630.83	422.17	400.18
	7.030	369.72	375.81	186.18	116.06	423.57	631.73	422.78	400.75
	7.040	370.25	376.35	186.45	116.23	424.17	632.62	423.38	401.32
	7.05	370.77	376.88	186.71	116.39	424.77	633.52	423.98	401.89
	7.10	373.40	379.56	188.04	117.22	427.79	638.02	426.98	404.74
	7.15	376.03	382.23	189.36	118.04	430.80	642.51	429.99	407.60
	7.20	378.66	384.90	190.69	118.87	433.81	647.00	433.00	410.45
	7.25	381.29	387.58	192.01	119.69	436.82	651.50	436.01	413.30
	7.30	383.92	390.25	193.34	120.52	439.84	655.99	439.01	416.15
	7.35	386.55	392.92	194.66	121.34	442.85	660.48	442.02	419.00
	7.40	389.18	395.59	195.98	122.17	445.86	664.97	445.03	421.85
	7.45	391.81	398.27	197.31	122.99	448.87	669.47	448.03	424.70
	7.50	394.44	400.94	198.63	123.82	451.89	673.96	451.04	427.55
	7.55	397.07	403.61	199.96	124.65	454.90	678.45	454.05	430.40
	7.60	399.70	406.29	201.28	125.47	457.91	682.95	457.05	433.25
	7.65	402.33	408.96	202.61	126.30	460.92	687.44	460.06	436.10
	7.70	404.96	411.63	203.93	127.12	463.94	691.93	463.07	438.95
	7.75	407.59	414.30	205.25	127.95	466.95	696.43	466.07	441.80
	7.80	410.22	416.98	206.58	128.77	469.96	700.92	469.08	444.65
	7.85	412.85	419.65	207.90	129.60	472.97	705.41	472.09	447.50
	7.90	415.48	422.32	209.23	130.42	475.99	709.91	475.10	450.35
	7.95	418.10	425.00	210.55	131.25	479.00	714.40	478.10	453.20
	8.00	420.73	427.67	211.87	132.07	482.01	718.89	481.11	456.05
Allowable Limit		S	SPL	SPL	SPL	SPL	SPL	S	SPL
		421.05	631.58	631.58	631.58	631.58	631.58	421.05	631.58

Figure 28: Elastic Stress Analysis Results

The maximum allowable internal pressure for which the cylinder will safe is found to be 7.0014 MPa as per elastic stress analysis approach.

5.3.3 Limit Load Analysis (Elastic Perfectly Plastic Method)

In limit load analysis, a calculation is performed to find the lower bound of the maximum permissible internal pressure for which the pressure vessel won't collapse.

In order to determine the limit load of the pressure vessel, five times the hydrostatic test pressure, 12.25 MPa, is applied. The limit load is defined as the load for which large deformation will occur.

The solver is able to solve for the stress values up to the yield limit of the material. After the yield limit, the material will start flowing indefinitely since the value of the tangent modulus is taken as 0. The solver is unable to solve for convergence due to this infinite deformation of the material. This condition is referred to as a numerical convergence for the limit load. This value of limit load is then multiplied by a factor of

1.5 which is then defined as the burst pressure required for the plastic collapse of the pressure vessel.

Table 14: Pressure Loading for Elastic Plastic Analysis

Steps	Time, s	Pressure, MPa
1	0	0
1	1	3
2	2	12.25
3	3	0

The pressure load is applied in three steps as shown in the Table 14. The Figure 29 shows the graph for the Table 14.

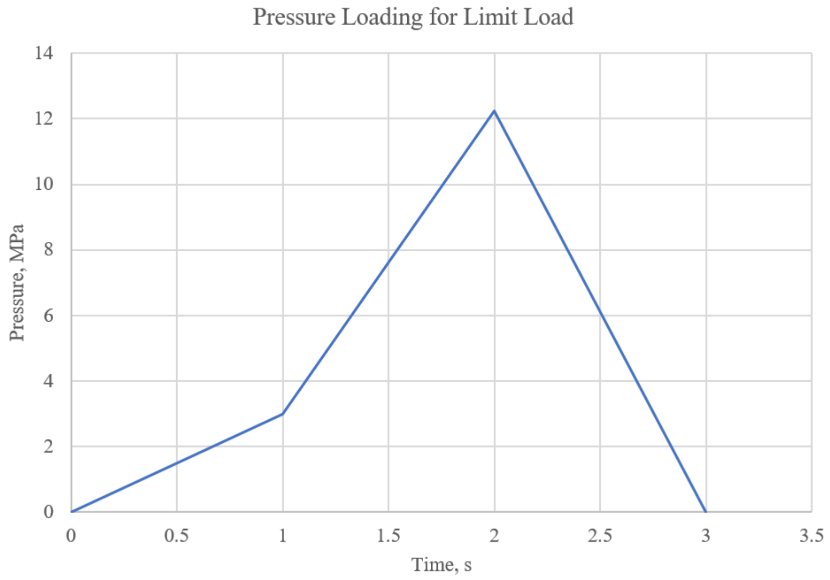

Figure 29: Pressure Load for Limit Load Analysis

The Figure 30 shows the plot of the equivalent stress obtained for the above pressure loading. The maximum equivalent stress obtained is 283.88 MPa which is the yield strength of the cylinder. The time at which the deformation grow indefinitely is about 1.2167 s. During this time, a pressure of about 5.004475 MPa is being applied to the cylinder.

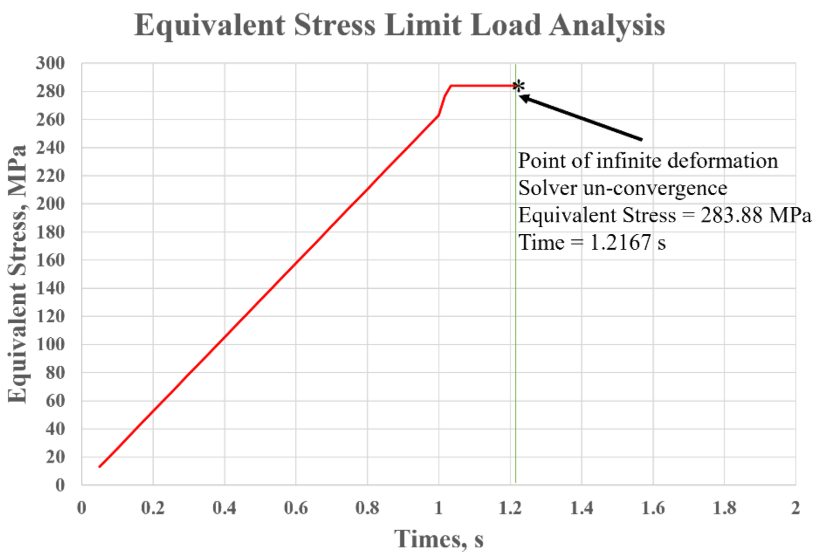

Figure 30: Equivalent Stress (Limit Load Analysis)

Also, a contour plot of equivalent stress obtained from the limit load analysis is presented in the Figure 31.The Figure shows the regions where the stress reaches the maximum allowable yield strength.

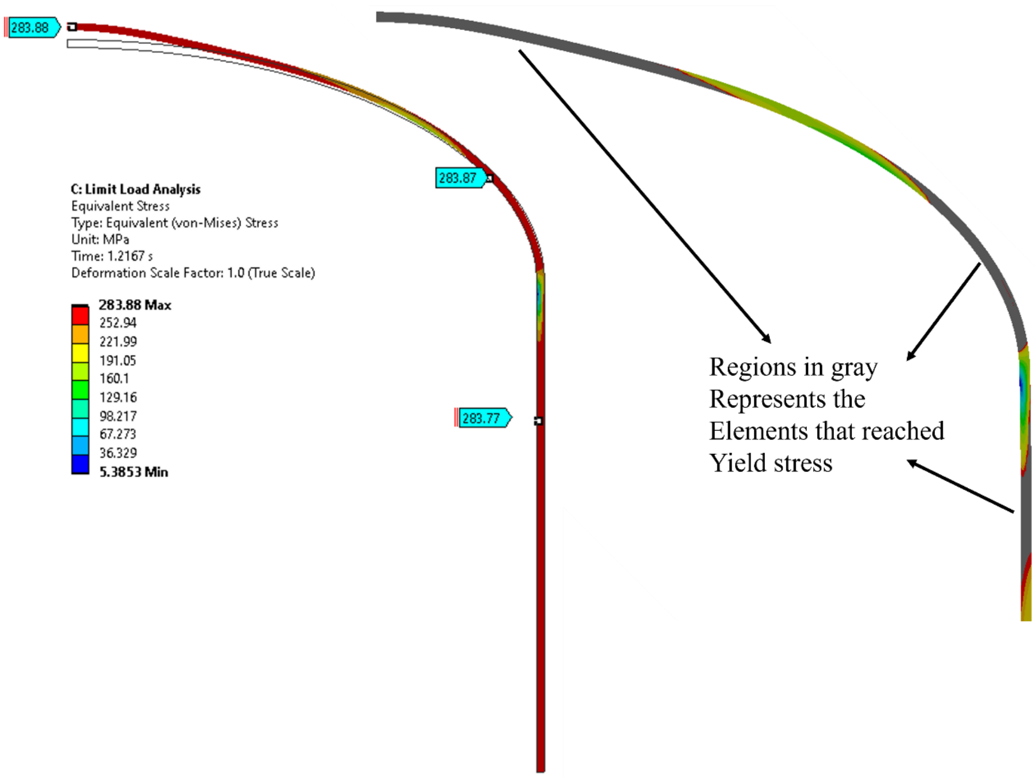

Figure 31: Limit Load Yield Location

Now, in order to determine the burst pressure from the limit load analysis method, the limit load pressure is multiplied with a factor of 1.5. Thus, from the limit load analysis, the burst pressure calculated is about 7.506713 MPa. The result and analysis for the limit load is demonstrated in the Table 15.

Table 15: Limit Load Results

Hydrostatic Test Pressure [MPa]	Minimum Required Burst Pressure [MPa]	Diverged Limit Load Pressure [MPa]	Burst Pressure Obtained [MPa]
2.45	3.68	5.004475	7.506713

5.3.4 Elastic Plastic Analysis

In this section, elastic-plastic analysis method is used to demonstrate the protection of the LPG cylinder against the plastic collapse. This method ensures that the cylinder can withstand the stress levels beyond elastic limits without catastrophic failure. For the protection against plastic collapse, a multilinear isotropic elastic plastic material behavior is used as per ASME BPVC, Division 2, Part 5.2.4.

The internal pressure loading is applied at the inner surface of the cylinder for one step. For time = 0 sec, 0 MPa is applied and for time = 1 sec, 20 MPa is applied. At particular value of the internal pressure, the solver will be unable to find the converged solution. This internal pressure causes the overall structure instability and this particular value of the internal pressure is known as the burst pressure using the elastic plastic analysis. In Figure 32, true equivalent stress developed is plotted for the time.

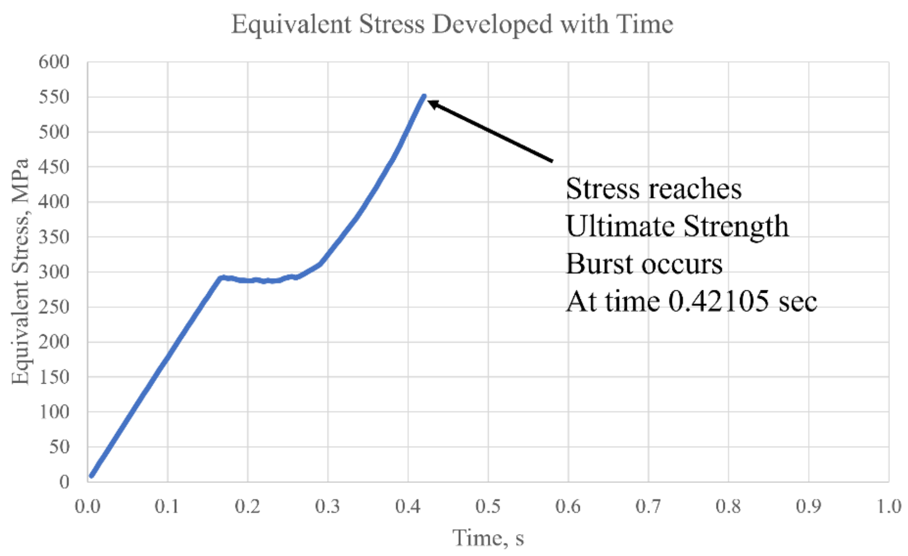

Figure 32: Equivalent Stress - Elastic Plastic Analysis

The plot of true equivalent stress at this time step is presented in the Figure 33.

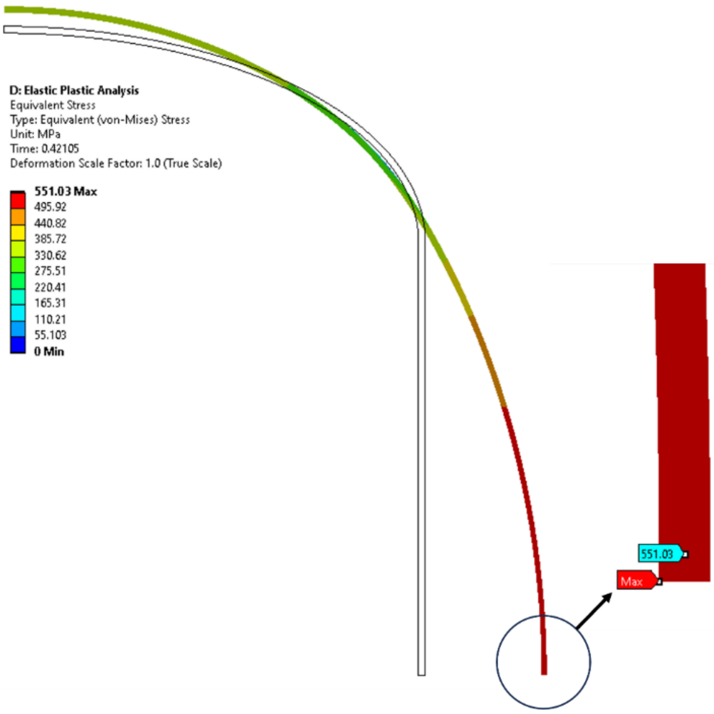

Figure 33: Equivalent Stress at 0.42105 sec - Elastic Plastic Analysis

The Figure 33 shows that the equivalent stress at the cylindrical portion becomes equal to the ultimate strength of the material at 0.42105 sec. Thus, after this time the LPG cylinder cannot withstand the internal pressure, thus resulting in the bursting of the cylinder. During this time, the following details are recorded as shown in the Table 16.

Table 16: Elastic Plastic Analysis Results

Time (s)	Equivalent Stress (MPa)	Burst Pressure (MPa)	Deformation (mm)	Plastic Strain (mm/mm)
0.42105	551.03	8.421	55.037	0.31681

5.4 Comparison of the Burst Pressure

The burst pressure obtained as per experimental, analytical and numerical simulation results is tabulated in the Table 17.

Table 17: Burst Pressure Comparison

Method	Burst Pressure (MPa)	Percentage Error
Experimental	8.72	-
Analytical	7	19.72
Elastic Analysis	7.0014	19.708
Limit Load Analysis	7.506713	13.91
Elastic Plastic Analysis	8.421	3.428

The Table 17 shows the experimental burst pressure obtained was 8.72 MPa which is greater than both the analytical and simulation burst pressure. Out of all the test methods, the burst pressure from the experimental test agrees with the burst pressure from the elastic plastic analysis with only 3.428% deviation.

Also, Table 8 and Table 10 shows the various stress components such as hoop stress and axial stress computed from the analytical solutions as well as from the numerical simulation using linear elastic method. The simulation results and the analytical solutions are in close agreement with each other.

The Figure 34 shows a plot of hoop and axial stress values for varying internal pressure using both the analytical and numerical simulation.

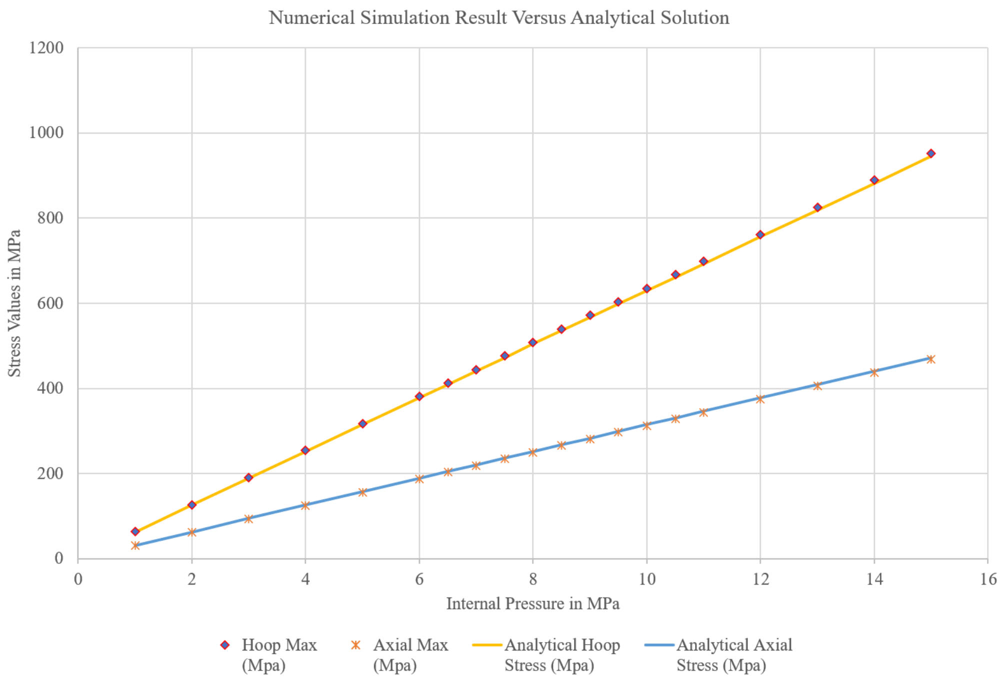

Figure 34: Numerical Simulation Result versus Analytical Solution

In the Figure 34, the straight lines represent the analytical stress values whereas the markers represent the simulation stress values for varying internal pressure.

5.5 Validation with Other Researches

The research done by Ozkan, Ozhan, and Genc (2019) show that out of all the three analysis approaches given by Design by Analysis, the elastic plastic analysis results the most non-conservative burst pressure. It overstimate the burst pressure as compared to the elastic and limit-load analysis. The same results are obtained in this research, i.e., the elastic plastic analysis yeilds the largest burst pressure among all other approaches.

Also, from the paper Bhatia and Mohammad (2019), the burst pressure from the simulation was 11.5 MPa while the average experimental burst pressure was 12 MPA for a cylinder wall thickness of 2.8mm. The yeild and ultimate strength considered is 265 MPa and 480 MPa. The results obtained from the research paper closely aggrees with the results obtained from Bhatia & Mohammad (2019).

5.6 Stress and Deformation Analysis at 8.421 MPa

The burst pressure obtained from the elastic plastic analysis is 8.421 MPa. So, an elastic-plastic analysis is run at this internal pressure to study the various stresses and deformations across the cylinder.

5.6.1 Equivalent Stress and Deformation

The Figure 35 shows two contour plots of equivalent von-mises stress for an internal burst pressure of 8.421 MPa. A maximum of 551.03 MPa is obtained at this burst pressure. The left contour shows the undeformed shape of the LPG cylinder whereas the right contour shows the true scale deformed shape of the LPG cylinder. The maximum equivalent stress occurs near the cylindrical portion of the LPG cylinder.

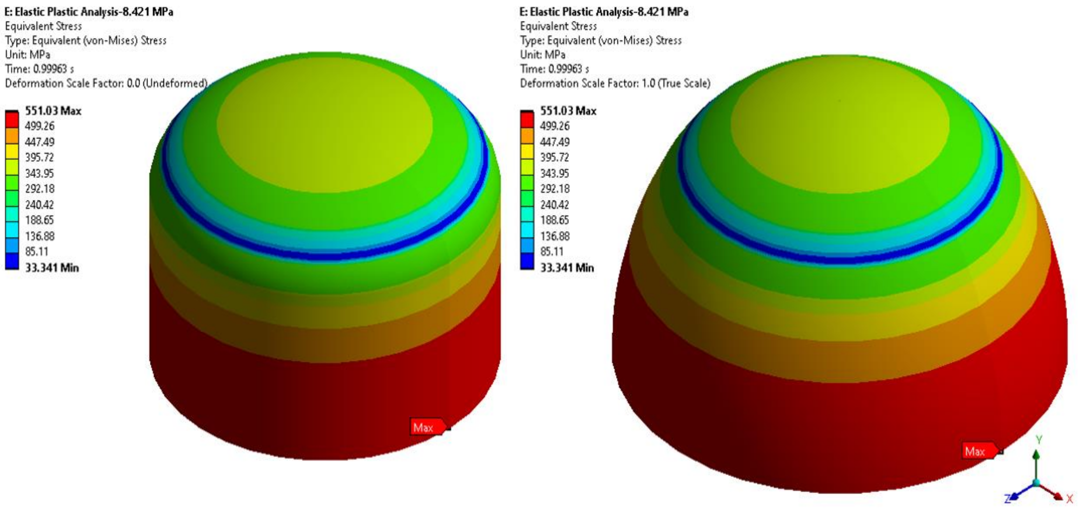

Figure 35: Equivalent Von-Mises Stress

The Figure 36 shows six different contour plots of equivalent stress plotted along the cross section of the LPG cylinder for different time step up until the bursting. The Figure shows the value of the time, the pressure at that particular instant, the maximum deformation and the maximum equivalent von-mises stress developed at that instant.

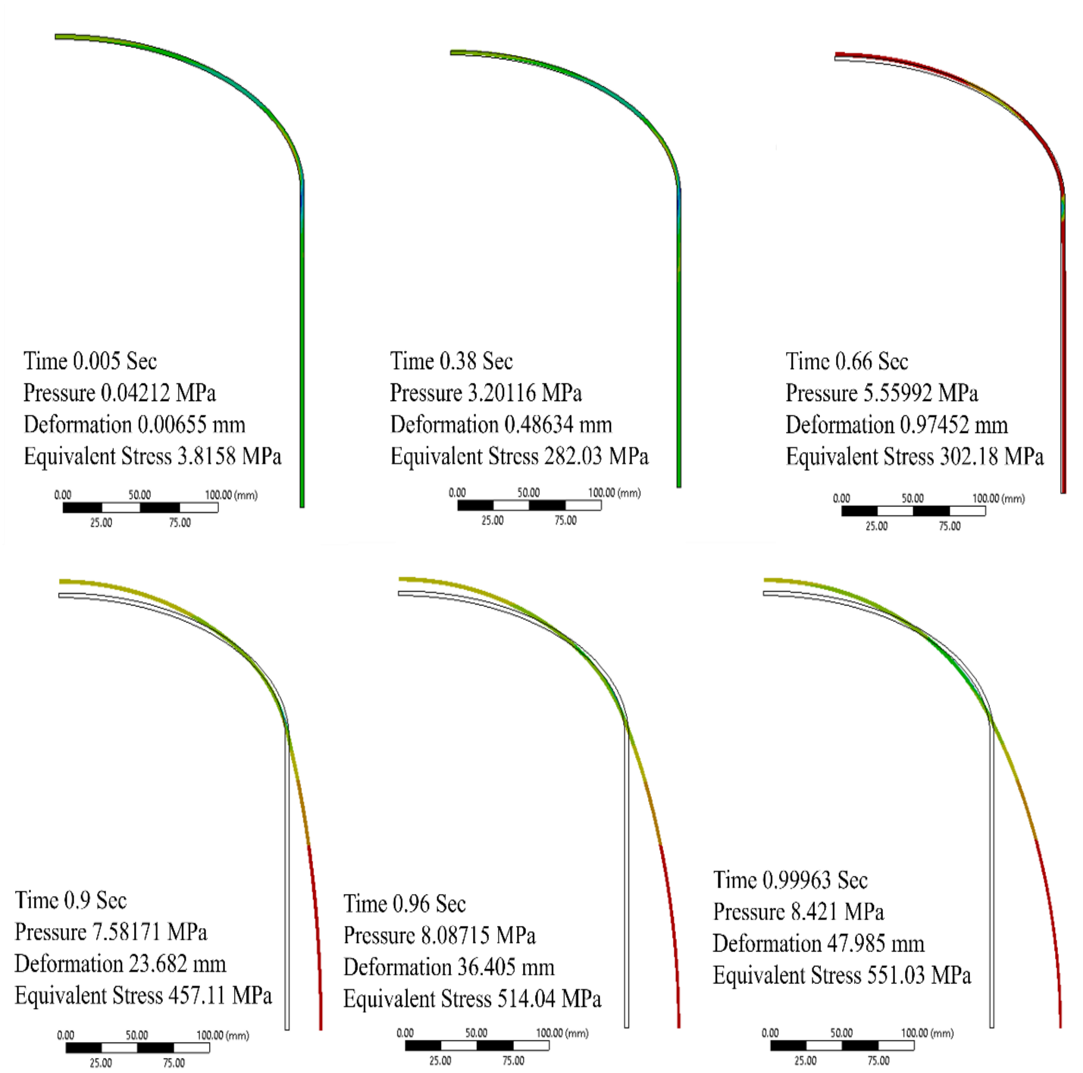

Figure 36: Equivalent Stress and Deformation for different time step

The Figure 37 shows the plot of equivalent von-mises stress plotted for different time-step up until the bursting of the LPG cylinder.

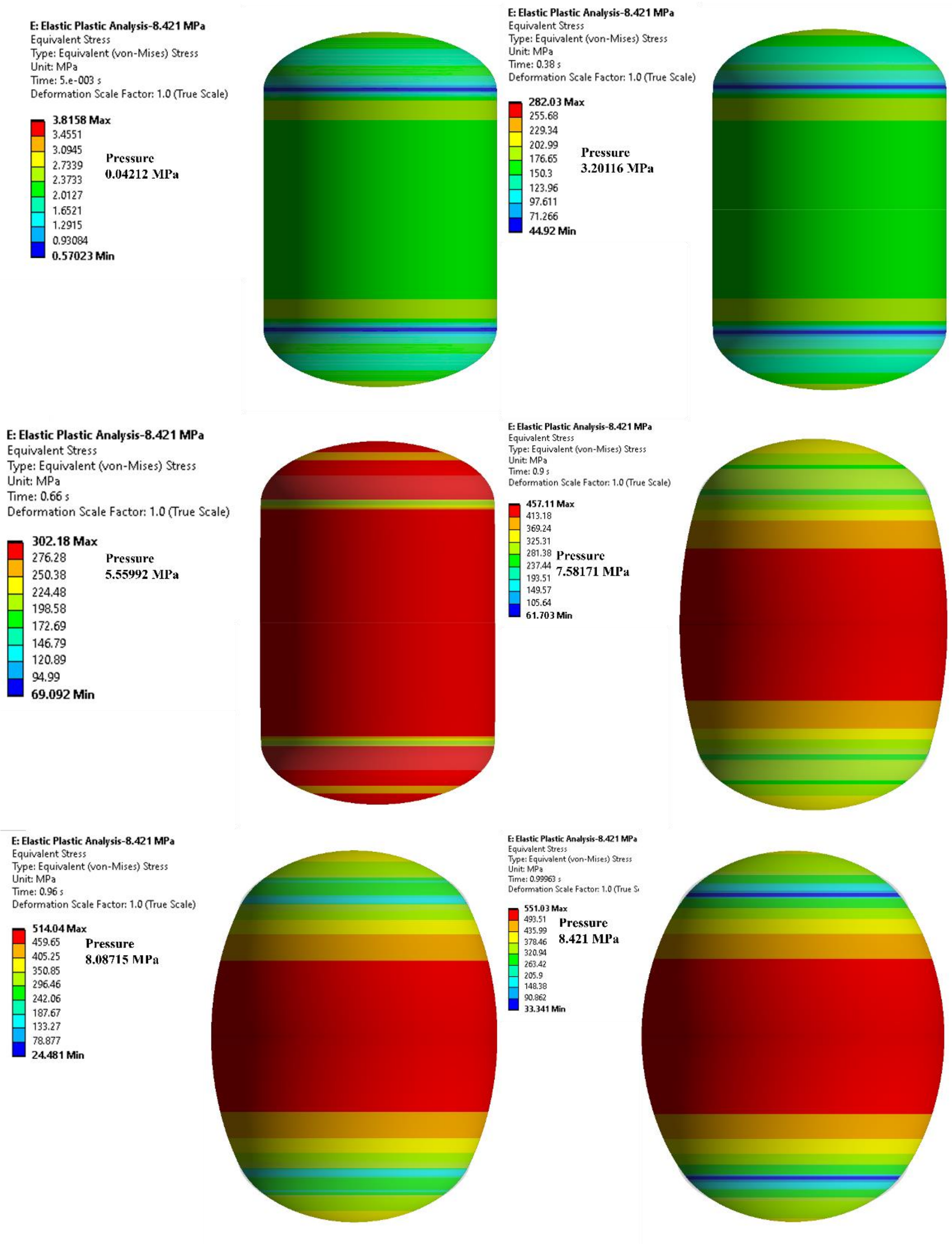

Figure 37: Development of Equivalent Von-Mises Stress until the Bursting

5.6.2 Hoop Stress

The Figure 38 shows a plot of hoop stress as shown where the maximum value obtained is 616 MPa. This value of the hoop stress is much greater than the value of the equivalent von-mises stress. As we know the hoop stress is one of the largest principal stresses present in the pressure vessels. It is important to consider hoop stress prior to the equivalent von-mises stress.

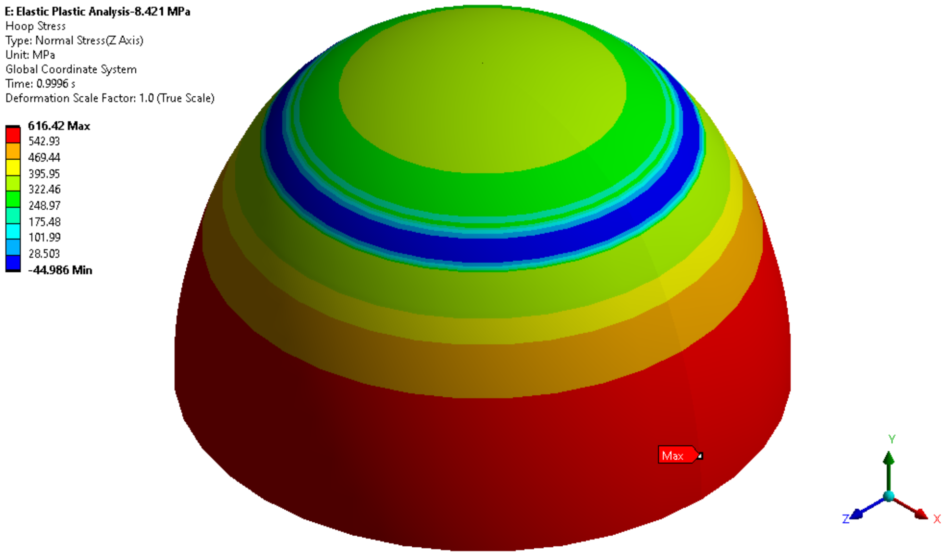

Figure 38: Hoop Stress

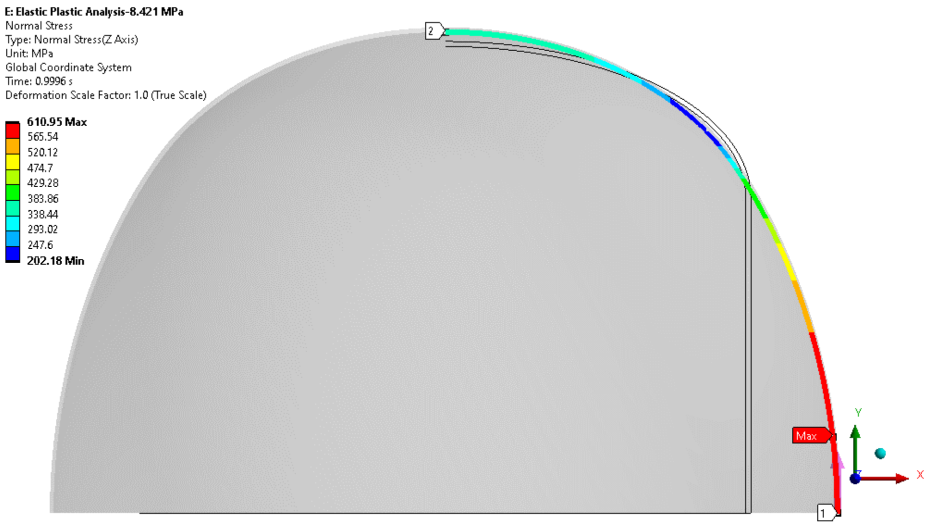

Figure 39: Hoop Stress along the Path 1-2

The Figure 39 shows the plot of hoop stress across the inner surface of the LPG cylinder as shown. Also, the Figure 40 shows the variation of the hoop stress along the path. The plot shows that near the point 1, the hoop stress is maximum and it gradually decreases till it reaches the shell and head juncture. And after that it grows till the crown of the ellipsoid.

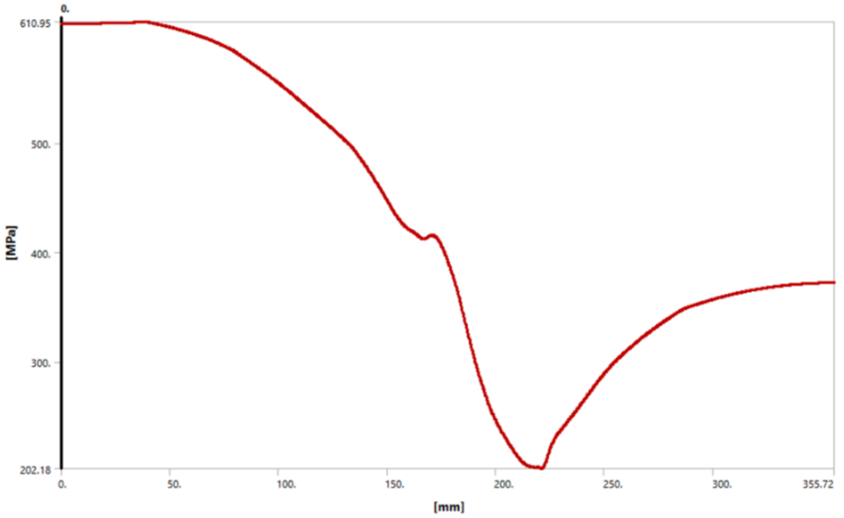

Figure 40: Hoop Stress Variation across the path 1-2.

5.6.3 Axial Stress

The Figure 41 shows the contour plot of the axial stress present in the LPG cylinder. The maximum axial stress present is near the base of the cylindrical portion as indicated by the color red. Here, the axial stress is not half of the hoop stress. The reason may be due to the non-linear material properties and also due to the bending effect of the shell and head juncture.

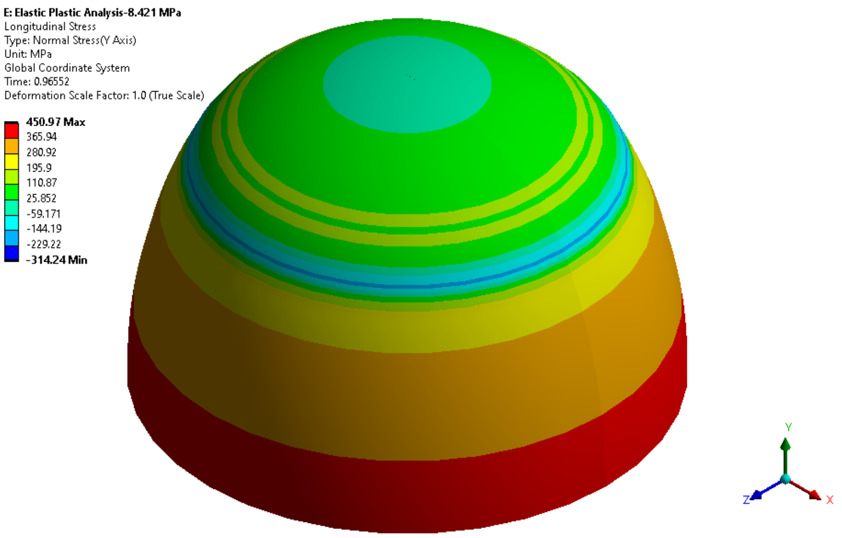

Figure 41: Axial Stress

CHAPTER SIX: CONCLUSION AND RECOMMENDATION

6.1 Conclusions

The burst strength analysis of the 14.2 Kg LPG cylinder is done. While doing so, different methods are employed to find the burst pressure of the LPG cylinder. First of all, hydrostatic burst pressure test is performed considering total of nine samples and from which **8.72** MPa is obtained as the experimental value of the burst pressure. A series of tensile test is also performed from which the yield strength, ultimate tensile strength and the % elongation at the fracture obtained are **283.879** MPa, **421.045** MPa and **36.611**%. The material properties of the structural steel used to manufacture the LPG cylinders confirms to the standards as per NS 367, 2053.

Similarly, the analytical solutions are calculated for the LPG cylinder with the assumptions of a thin-walled pressure vessel and from the analytical calculation using the shell theory, the burst pressure obtained was **6.98** MPa. Using ASME BPVC VIII, Division 1 and Nepal standards, the minimum internal pressure that the LPG cylinder could handle was calculated as **4.667** and **3.56** MPa. Here, the yield strength of **283.879** MPa is considered to be the allowable stress limit. Beyond these internal pressure values, the codes predicts that plastic deformation will occur.

Three different numerical simulation are performed as per ASME BPVC, Division 2, Part 5, Design by Analysis. The methods are elastic analysis, limit-load analysis, and elastic plastic analysis. Out of these three methods, elastic plastic analysis is the most realistic and practical one. **7.0014**, **7.506713**, and **8.421** MPa are the corresponding burst pressure values obtained from the elastic, limit-load, and elastic-plastic analysis. The burst pressure obtained from the elastic plastic analysis differs from the experimental burst pressure by **3.428%** thereby concluding that the elastic plastic approach to determine the burst pressure of the LPG cylinder to be most accurate than the other analysis approach.

The equivalent stress, hoop stress, and the axial stress are the most important stress components. Generally, the value of the equivalent von-mises stress is considered as a failure criterion in most of the solid mechanics problem. However, in the case of LPG cylinders, hoop stress is the most important stress component. At the burst pressure, the numerical simulation shows that the value of the hoop stress is much larger than the value of the equivalent von-mises stress. Thus, failure criteria in case of LPG cylinders can also be checked with the help of hoop stress. Also, the axial stress developed in the LPG cylinders are generally half the hoop stress values. At the burst pressure, the maximum hoop, axial and the equivalent von-mises stress developed are **611**, **450** and **551.03** MPa.

The LPG cylinders are safe as per Nepal Standards. The working pressure and the hydrostatic test pressure is generally considered to be **1.65** MPa and **2.45** MPa. From the research, a burst pressure of **8.421** MPa is found which is **3.43** times higher than the test pressure as per Nepal Standards and **five** times higher than the maximum working pressure inside the LPG cylinders.

6.2 Recommendations

1. The research does not consider the effect of the circumferential weld present in the LPG cylinder. Further research can be done studying the effect of the weld bead on the burst strength of the LPG cylinder.
2. The nozzle at the top of the ellipsoidal head is not considered while performing the numerical simulation. Simulations can be performed considering the nozzle shell opening and studying the stress concentration near that region and its effect on the burst strength of the LPG cylinder.
3. The LPG cylinders used may be worn out since they are continuously refilled and reused. Numerical simulations can be performed as per ASME BPVC, Protection against Fatigue to study the fatigue life of the LPG cylinders.
4. Since with the increase in temperature, the vapor pressure of the LPG increases. Further studies can be made to understand the effect of temperature variation on the vapor pressure of the LPG and the stresses developed with it.

REFERENCES

1 (2016, June 18). Retrieved from The Kathmandu Post: https://kathmandupost.com/money/2016/06/18/circulation-of-poor-quality-lpg-cylinders-puts-consumers-at-risk

2 (2018, January 5). Retrieved from The Himalayan Times: https://thehimalayantimes.com/business/nepal-bureau-of-standards-and-metrology-shut-gas-plants-flouting-safety-rules/

3 Abdussalam, R. M. (2006). *Finite Element Analysis of the Design and Manufacture of Thin-walled Pressure Vessels used as Aerosol Cans.*

4 Adolf, J., Balzer, C., Joedicke, A., & Schabla, U. (2015). *Shell LPG Study.* Shell Deutschland, Hamburg.

5 Aksoley, M. E., Ozcelik, B., & Bican, I. (2007). Comparison of bursting pressure results of LPG tank using experimental and finite element method. *Jounal of Hazardous Materials*.

6 Annaratone, D. (2007). *Pressure Vessel Design.* Springer.

7 ASME. (2023). *ASME Boiler and Pressure Vessel Code VIII - Div 1.*

8 ASME. (2023). *ASME Boiler and Pressure Vessel Code VIII - Div 2.*

9 Barlow, P. (1836). On the Strength of Hydrostatic Presses. In P. Barlow, *A Treatise on the Strength of Timber, Cast Iron, Malleable Iron, and Other Materials.*

10 Barrett, S. L. (n.d.). *Hoop, Axial, and Radial Stresses in Thick-Walled Pressure Vessels.* Retrieved from Ansys: https://courses.ansys.com/index.php/courses/stresses-in-pressure-vessels/

11 Bhatia, P., & Mohammad, D. A. (2019). LPG Tank Burst Pressure Determination using FEM. *IRJET*.

12 Brabin, T. A., Christopher, T., & Rao, B. N. (2011). Bursting Pressure of Mild Steel Cylindrical Vessels. *International Journal of Pressure Vessels and Piping*, 119-122.

13 Brownell, L. E., & Young, E. H. (1959). *Process Equipment Design.* John Wiley & Sons, Inc.

14 Christopher, T., Sarma, B. S., Potti, P. K., Rao, B. N., & Sankarnarayansamy, K. (2002). A comparative study of failure pressure estimations of unflawed cylindrical vessels. *International Jounal o f Pressure Vessels and Piping*.

15 Dharmarao, S. S. (2015). Design and Analysis of Thick Pressure Vessels.

16 Doane, J. (2018). Pressure Vessels. In *Thin and Thick-Walled Stress Analysis* (p. 31).

17 Fadel, A. H., & Yahya, N. A. (2021). Experimentally Determination of Burst Pressure and Failure Location of Liquefied Petroleum Gas Cylinder. *University Bulletin, 4*(23).

18 Harvey, F. J. (1985). *Theory and Design of Pressure Vessels* (1 ed.). New York, United States of America: Van Nostrand Reinhold Company.

19 Hazizi, K., & Ghaleeh, M. (2023). Design and Analysis of a Typical Vertical Pressure Vessel Using ASME Code and FEA Technique. *Designs*.

20 Jegatheesan, J., & Zakaria, Z. (2018). Stress Analysis on Pressure Vessel. *Environment & Ecosystem Science*.

21 Kaptan, A., & Kisioglu, Y. (2007). Determination of burst pressures and failure locations of vehicle LPG cylinders. *Pressure Vessels and Piping*.

22 Kisioglu, Y. (2009). Burst tests and volume expansions of vehicle toroidal LPG fuel tanks. *Turkish J. Eng. Env. Sci.*

23 Li, H., Huang, X., Yang, P., & Yang, H. (2017). A new pressure vessel design by analysis method avoiding stress catetgorization. *International Journal of Pressure Vessels and Piping*.

24 Macwan, S. P., & Hu, Z. (2011). Experimental Verification of Model Pressurized Thick-Walled Cylinder with Numerical and Theoretical Methods. *International Mechanical Engineering Congress & Exposition*.

25 Magar, H. K., Basnet, K. B., & Ghimire, L. (2023). *Using DEAL.II for Structural analysis of a Medical Oxygen Cylinder.*

26 Mohamed, A. F. (2018). Finite Element Analysis for Stresses in ThinWalled Pressurized Steel Cylinders. *International Journal of Scientific & Engineering*.

27 Moss, D. (2004). *Pressure Vessel Design Manual* (Third ed.). Elsevier.

28 Moss, D., & Basic, M. (2013). *Pressure Vessel Design Manual* (Fourth ed.). Elsevier.

29 Oh, D. H., Race, J., Oterkus, S., & Chang, E. (2020). A New Methodology for the Prediction of Burst Pressure for API 5L X Grade Flawless Pipelines. *Ocean Engineering*.

30 Ozkan, H. H., Ozhan, S., & Genc, G. (2019). Analysis and Design of Hemispherical Head Pressure Vessel. *Afyon Kocatepe University International Journal of Engineering Technology and Applied Sciences*.

31 Palanivelu, P., & Prasad, R. S. (2017). A Paper on Design and Analysis of Pressure. *International Journal of Engineering Research & Technology (IJERT)*.

32 Patil, A. D., & Jadhav, M. M. (2017). Analysis of Pressure Vessel: A Review. *International Journal for Innovative Research in Science & Technology*.

33 Post, T. K. (2023, February 17). *The Kathmandu Post.* Retrieved 6 1, 2024, from https://kathmandupost.com/national/2023/02/17/as-accidents-rise-concerns-grow-over-safety-of-cooking-gas-cylinders

34 Ramakrishna, A., Siddiqui, N. A., & Lal, P. S. (2013). Study on Hydro Testing of LPG Cylinders. *IJEIT*.

35 Rangari, L. D., Zode, P. M., & Mehar, P. (2012). Finite Element Analysis of LPG Gas Cylinder. *International Journal of Applied Research*.

36 Setiyo, M., Soeparman, S., Hamidi, N., & Wahyudi, S. (2017). Characteristic Of LPG Compositions in the Fuel Line During Discharging Process. *International Journal of Technology*, 112-121. doi:10.14716/ijtech.v8i1.4117

37 Standard, I. (2010). *Welded Low Carbon Steel Cylinders Exceeding 5 Litre Water Capacity For Low Pressure Liquefiable Gases.* Burea of Indian Standards.

38 Standard, N. (2074). *Specification for LPG Cylinders Exceeding 5 liter up to 250 liter Water Capacity.* Nepal Burea of Standards and Metrology.

39 Standards, I. (2010). *Liquified Petroleum Gas (LPG) - Specification.* Burea of Indian Standards.

40 Standards, N. (2074). *Test Methods for LPG Cylinders.* Nepal Burea of Standards.

41 (n.d.). *Technical Data for Propane, Butane, and LPG Mixtures.* Alternate Energy Systems, Inc.

42 Thubrikar, M. J. (2007). Pressure Vessel Principles. In M. J. Thubrikar, *Vascular Mechanics and Pathology* (pp. 82-106). Springer.

43 Turner, L. B. (1910). The stresses in a thick hollow cylinder subjected to internal pressure.

44 Ugochukwu, C., Oluwole, O., & Odunfa, K. (2018). Finite Element Analysis of Displacement and Von-Mises Stress in Cylindrical Liquified Petroleum Gas Pressure Tank. *Covenant Journal of Engineering Technology*.

45 Wadkar, V. V., S. S. Malgave, D. D., & H. S. Bhore, P. P. (2015). Design and Analysis of Pressure Vessel Using Ansys. *Journal of Mechanical Engineering and Technology*.

46 Wang, H., Yao, X., Li, L., Sang, Z., & Krakauer, B. W. (2017). Imperfection sensitivity of externally-pressurized, thin-walled, torispherical-head buckling. *Thin-Walled Structures*.

47 Wang, H., Zheng, T., Sang, Z., & Krakauer, B. W. (2021). Burst Pressures of thin-walled cylinders constructed of steel exhibiting a yield plateau. *International Journal of Pressure Vessels and Piping*.

48 Wibawa, L. A. (2020). Numerical Study Of The Effect Of Wall Thickness And Internal Pressure On Von Mises Stress And Safety Factor Of Thin-Walled Cylinder For Rocket Motor Case. *Jurnal Sains dan Teknologi*.

49 Yahya, N. A., Daas, O. M., Alboum, N. O., & Khalile, A. H. (2018). Design of Vertical Pressure Vessel Using ASME Codes. *Engineering Sciences and Technology*.

50 Yin, Z., Su, T., & He, M. (2019). Gas Packaging Container Based on ANSYS Finite Element Analysis and Structural Optimization Design. *Journal of Physics: Conference Series*.

51 Zhou, M., Patel, A., Wang, B., Jin, W., & Li, Y. (2021). Design Optimization of Pressure Vessel in Compliance With Elastic Stress Analysis Criteria for Plastic Collapse Using an Integrated Approach. *Journal of Pressure Vessel Technology*.

52 Zhu, X.-K., Wiersma, B., Johnson, W. R., & Sindelar, R. (2023). Burst Pressure Solutions of Thin and Thick-Walled Cylindrical Vessels. *Journal of Pressure Vessel Technology*.

APPENDIX A: STANDARDS AND CODES

Nepal Standards

The following formulas are used to determine the wall thickness of the pressure vessels as per Nepal Standards.

1. Calculation of the cylindrical shell thickness:

1
$$t = \frac{P_h D_o}{200 \times 0.8 J R_e + P_h} \quad \text{A.1}$$

2
$$t = \frac{P_h D_i}{200 \times 0.8 J R_e - P_h} \quad \text{A.2}$$

3
$$t = 0.136 \times \sqrt{D_o} \quad \text{A.3}$$

The greater values between A.1, A.2, and A.3 should be selected for the cylindrical shell thickness.

a. Calculation of the tori-spherical head thickness:

$$t = \frac{P_h D_o}{200 \times 0.8 J R_e + P_h} \times \frac{KZ}{5} \quad \text{A.4}$$

b. Calculation of the semi-ellipsoidal head thickness:

$$t = \frac{P_h D_o}{200 \times 0.8 J R_e + P_h} \times \frac{K(0.65 + 0.1K)}{4} \quad \text{A.5}$$

The schematic of the semi-ellipsoid is provided in the Appendix A 1.

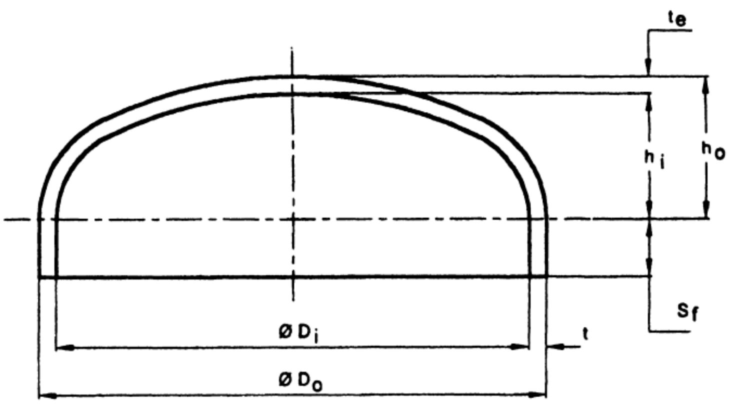

Appendix A 1: Schematic of Semi-Ellipsoidal Head

ASME BPVC Design by Rule (DBR)

For the thickness of the pressure vessels under internal pressure, UG-27 can be used for the cylindrical shells and ellipsoidal heads can be used as given by ASME BPVC Division 1.

1. Cylindrical Shells:

   When the thickness of the cylindrical pressure vessel does not exceed one-half of the inside radius or the internal pressure does not exceed 0.385 times the allowable stress limit, the following formula can be used:

   1. $$P_{\text{cylinder, Circumferential Stress}} = \frac{S \times E \times t}{R + 0.6 \times t} \tag{A.6}$$

   2. $$P_{\text{cylinder, Longitudinal Stress}} = \frac{S \times E \times t}{R - 0.4 \times t} \tag{A.7}$$

2. Ellipsoidal Heads:

   The internal pressure and thickness of the head can be determined using the formula as:

   3. $$P_{\text{Ellipsoidal}} = \frac{2 \times S \times E \times t}{D + 0.2 \times t} \tag{A.8}$$

These formulas can be used to calculate the internal pressure and the wall thickness when the allowable stress limit and joint efficiency are known.

The Appendix A 2 shows the stress categories and the limits of equivalent stress as per elastic analysis approach.

Figure 5.1
Stress Categories and Limits of Equivalent Stress

Stress Category	Primary			Secondary Membrane plus Bending	Peak
	General Membrane	Local Membrane	Bending		
Description (For examples, see Table 5.2)	Average primary stress across solid section. Excludes discontinuities and concentrations. Produced only by mechanical loads.	Average stress across any solid section. Considers discontinuities but not concentrations. Produced only by mechanical loads.	Component of primary stress proportional to distance from centroid of solid section. Excludes discontinuities and concentrations. Produced only by mechanical loads.	Self-equilibrating stress necessary to satisfy continuity of structure. Occurs at structural discontinuities. Can be caused by mechanical load or by differential thermal expansion. Excludes local stress concentrations.	1. Increment added to primary or secondary stress by a concentration (notch). 2. Certain thermal stresses which may cause fatigue but not distortion of vessel shape.
Symbol	P_m	P_L	P_b	Q	F

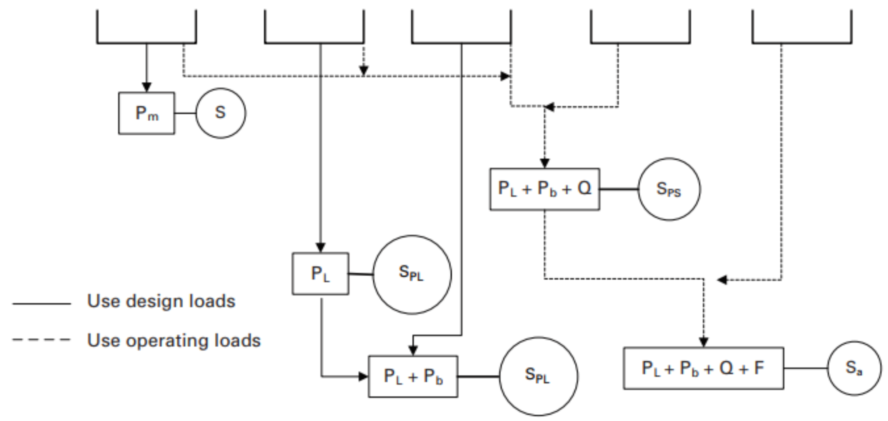

Appendix A 2: Stress Categorization and Limits of Equivalent Stress used in the Elastic Analysis

[Image Source: ASME BPVC Section VIII Division 2 Figure 5.1]

The Appendix A 3 shows the classification of stresses that can be used while using the elastic analysis approach.

Table 5.6
Examples of Stress Classification

Vessel Component	Location	Origin of Stress	Type of Stress	Classification
Any shell including cylinders, cones, spheres, and formed heads	Shell plate remote from discontinuities	Internal pressure	General membrane	P_m
			Gradient through plate thickness	Q
		Axial thermal gradient	Membrane	Q
			Bending	
	Near nozzle or other opening	Net-section axial force and/ or bending moment applied to the nozzle, and/ or internal pressure	Local membrane	P_L
			Bending	Q
			Peak (fillet or corner)	F
	Any location	Temperature difference between shell and head	Membrane	Q
			Bending	
	Shell distortions such as out-of-roundness and dents	Internal pressure	Membrane	P_m
			Bending	Q
Cylindrical or conical shell	Any section across entire vessel	Net-section axial force, bending moment applied to the cylinder or cone, and/or internal pressure	Membrane stress averaged through the thickness, remote from discontinuities; stress component perpendicular to cross section	P_m
			Bending stress through the thickness; stress component perpendicular to cross section	P_b
	Junction with head or flange	Internal pressure	Membrane	P_L
			Bending	Q
Dished head or conical head	Crown	Internal pressure	Membrane	P_m
			Bending	P_b
	Knuckle or junction to shell	Internal pressure	Membrane	P_L [Note (1)]
			Bending	Q
Flat head	Center region	Internal pressure	Membrane	P_m
			Bending	P_b
	Junction to shell	Internal pressure	Membrane	P_L
			Bending	Q [Note (2)]

Appendix A 3: Stress Classification
[Image Source: ASME BPVC Section VIII Division 2 Table 5.6]

APPENDIX B: LPG DETAILS

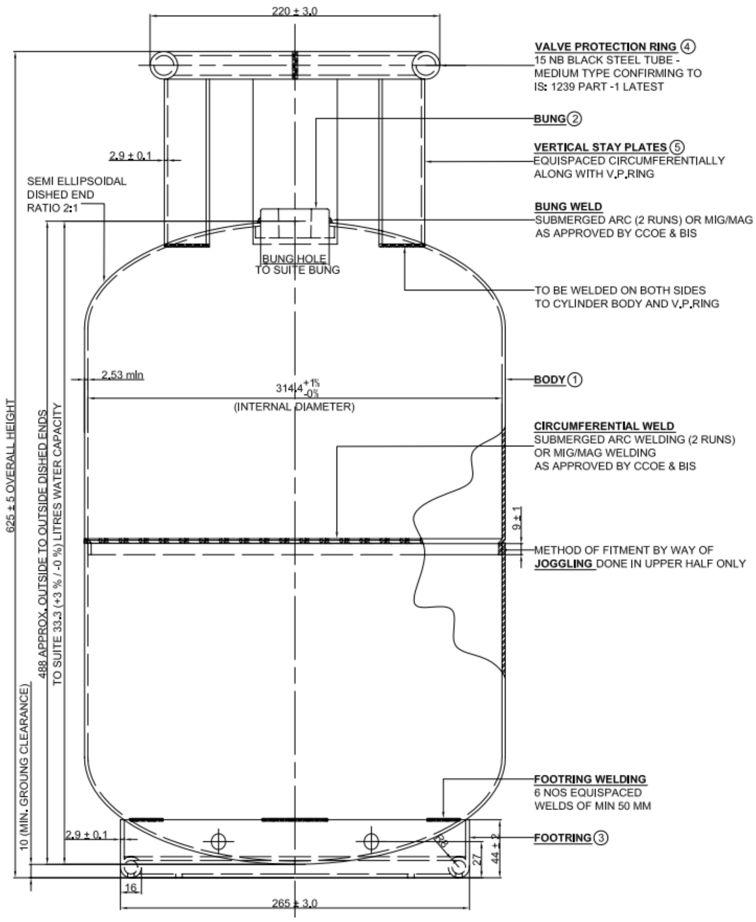

Appendix B 1: Drawing of 14.2 Kg LPG Cylinder

[source: Bharat Petroleum Corporation Limited]

Properties of Outline Row 3: Low Carbon Structural Steel EP Material

	A	B	C	D	E
1	Property	Value	Unit		
2	Material Field Variables	Table			
3	Isotropic Elasticity				
4	Derive from	Young's Modulus a...			
5	Young's Modulus	200	GPa		
6	Poisson's Ratio	0.3			
7	Bulk Modulus	1.6667E+11	Pa		
8	Shear Modulus	7.6923E+10	Pa		
9	Multilinear Isotropic Hardening	Tabular			
10	Scale	1			
11	Offset	0	MPa		
12	Tensile Yield Strength	283	MPa		
13	Compressive Yield Strength	283	MPa		
14	Tensile Ultimate Strength	421.05	MPa		
15	Compressive Ultimate Strength	421.05	MPa		

Appendix B 2: Material Details in ANSYS Engineering Data for Elastic-Plastic Analysis

APPENDIX C: IMAGES FROM THE EXPERIMENTS

Appendix C 1: Test Specimen cut out from the LPG Cylinder Sample (P samples)

Appendix C 2: Prepared Test Specimen PT and PL for Tensile Test as per Nepal Standards

Appendix C 3: Layout of the Test Specimen W for Tensile Test

Appendix C 4: Tensile Test Process

Appendix C 5: Figure Showing Test Specimen before and after Tensile Test. A Gage length of 50 mm is taken.

Appendix C 6: Measurement of elongated gage length after the tensile test

Appendix C 7: Bending Test done as per acceptance test stated in the Nepal Standards

Appendix C 8: Measurement of Tare weight of the LPG Cylinder

plagiarismCheckChandra_076MSMDE005.docx

ORIGINALITY REPORT

14%

SIMILARITY INDEX

PRIMARY SOURCES

1	www.bis.org.in Internet	123 words — 1%
2	Kristaq Hazizi, Mohammad Ghaleeh. "Design and Analysis of a Typical Vertical Pressure Vessel Using ASME Code and FEA Technique", Designs, 2023 Crossref	86 words — 1%
3	cae-cube.ru Internet	83 words — < 1%
4	dergipark.org.tr Internet	76 words — < 1%
5	Dominic J. Bello, Frederick A. Leckie. "Strength and Stiffness of Engineering Systems", Springer Nature, 2009 Crossref	73 words — < 1%
6	www.science.gov Internet	67 words — < 1%
7	Donatello Annaratone. "Pressure Vessel Design", Springer Science and Business Media LLC, 2007 Crossref	64 words — < 1%
8	Do Han Oh, Julia Race, Selda Oterkus, Enrong Chang. "A new methodology for the prediction of	58 words — < 1%